

**Performance Analysis of the MC-CDMA System in Frequency
Selective Slow Rayleigh Fading Channels, DS-CDMA or MC-
CDMA?**

T.H. Lee

DELFT UNIVERSITY OF TECHNOLOGY

Department of Electrical Engineering

Telecommunication and Traffic-Control Systems Group

Title: **Performance analysis of the MC-CDMA system in frequency selective
slow Rayleigh fading channels, DS-CDMA or MC-CDMA?**

Author: T.H. Lee

Type : Graduation report

Size : vii + 62

Date : October 23, 1995

Mentors: Prof. Dr. R. Prasad
Dr. S. Hara (Osaka University, Japan)
Code: A-684
Period: March 95- September 95

Abstract

This report describes the Bit Error Probability (BEP) performance of Multi-Carrier Code Division Multiple Access (MC-CDMA) system using the RAKE-receiver in frequency selective slow Rayleigh fading channels. The analysis has been carried out by a theoretical approach using the characteristic function method for quadratic form of Gaussian random variables and by computer simulation. The BEP performance of Direct Sequence Code Division Multiple Access (DS-CDMA) system under the same conditions is analysed and compared with the BEP performance of the MC-CDMA system.

Indexing terms: Digital Communication, Spread Spectrum, Code Division Multiple Access, Multi-Carrier Code Division Multiple Access

Summary

Multi-Carrier Code Division Multiple Access (MC-CDMA) is a new protocol. It was proposed by Linnartz et al. in 1993. The MC-CDMA protocol is based on spread spectrum technique. In the MC-CDMA system the signal is spread by using a number of subcarriers and orthogonal codes.

One of the serious problems in wireless radio communications is multipath fading, which severely degrades the system performance. This phenomenon can be combated by using MC-CDMA. We analyse the BEP performance of the MC-CDMA system in frequency selective slow Rayleigh fading channels. The results of this analysis are compared with the BEP performance of a well-known Direct Sequence Code Division Multiple Access (DS-CDMA) system. Also, it will be compared under the same conditions: the same kinds of Power Delay Profile (PDP) and RAKE structures are used in both CDMA receivers, that is, the frequency domain RAKE-receiver for the MC-CDMA system and the time domain RAKE-receiver for the DS-CDMA system. In order to take the correlation of subcarriers into account an exponential PDP is assumed and the result is compared with that using a uniform PDP, which is equal to the case where the subcarriers are uncorrelated. The analysis is done theoretically and by using computer simulation. The BEP lowerbound is obtained by using the characteristic function method for quadratic form of Gaussian random variables. Unfortunately there is no closed form for the BEP upperbound for the MC-CDMA system, therefore, we have to resort to computer simulation. Also multiuser interference on the BEP performance for MC-CDMA system is analysed by using computer simulation because of its theoretical complexity. In addition a simple multiuser detection scheme is proposed.

The BEP lowerbounds for the MC-CDMA system obtained by theoretical and computer simulation agree well. From the BEP lowerbounds of the MC-CDMA and DS-CDMA systems we can conclude that the MC-CDMA system can outperform the DS-CDMA under certain circumstances. The BEP upperbound appears to be independent of the number of simultaneous users. Further we can see the MC-CDMA system can accommodate more users than the DS-CDMA system given a certain bandwidth.

List of symbols

$a_n[p]$	the p th bit of the data sequence
$\alpha_n(t)$	attenuation of the signal component at delay $\tau_n(t)$ for the n th path
B_d	Doppler spread
β_l	gain of the l th path
Δ	guard duration
$(\Delta f)_c$	coherence bandwidth
$c(\tau; t)$	lowpass channel function
$C(f; t)$	Fourier transform of $c(\tau; t)$
D	decision variable
$d_{n,k}$	Walsh-Hadamard code sequence of the n th user
Δf	frequency separation between two signals
f_c	the carrier frequency
$H(f)$	transfer function of a channel
$h(t)$	impulse response function of a channel
$\phi_c(\tau)$	multipath intensity profile or the delay power spectrum
$\phi_c(\tau, \Delta t)$	autocorrelation of $c(\tau, t)$
ϕ_k	random variable of the phases
K_{DS}	processing gain of DS-CDMA system
K_{MC}	processing gain of the MC-CDMA system
\mathbf{M}	covariance matrix
$P_{tb}(t)$	a unit pulse that is non-zero in the interval of 0 and T_b
R_k	random variable of the amplitude
$\mathbf{r}(t)$	received signal
$\rho_{x,y}$	complex correlation coefficient of random variables x and y
$s(t)$	transmitted signal
T_b	bit duration
T_m	multipath spread or rms delay spread
T_s	symbol duration
$\tau_n(t)$	delay for the n th path

W	bandwidth of the baseband signal
X_k	inphase phase component of R_k
Y_k	quadrature phase components of R_k

List of abbreviations

BEP	Bit Error Probability
BPSK	Binary Phase Shift Keying
CDMA	Code Division Multiple Access
DS-CDMA	Direct Sequence Code Division Multiple Access
IID	Independent and Identically Distributed
ISI	Intersymbol Interference
LOS	Line-Of-Sight
MC-CDMA	Multi-Carrier Code Division Multiple Access
MPD	Measured Power Delay
MRC	Maximum Ratio Combining
PDP	Power Delay Profile
pdf	probability density function
PN	Pseudorandom Noise
QPSK	Quadrature Phase Shift Keying
SS	Spread Spectrum
WH	Walsh-Hadamard
WSS	Wide Sense Stationary
WSSUS	Wide Sense Stationary Uncorrelated Scattering
US	Uncorrelated Scattering

CONTENTS

Summary	i
List of symbols.....	ii
List of abbreviations.....	iv
1 Introduction.....	1
2 Multipath Fading Channel.....	5
2.1 Multipath fading.....	5
2.1.1 Delay spread and coherence bandwidth.....	7
2.2.2 Doppler spread and coherence time.....	9
2.2 Diversity techniques.....	9
3 MC-CDMA and DS-CDMA Systems.....	11
3.1 MC-CDMA system	12
3.1.1 Base station model	12
3.1.2 Channel model	14
3.1.3 Receiver model	15

3.2 DS-CDMA system	16
3.2.1 Base station model	17
3.2.2 Channel model	18
3.2.3 Receiver model	19
3.2 Design of the systems	20
4 BEP Performance Analysis.....	21
4.1 BEP analysis for the MC-CDMA.....	21
4.1.1 BEP lowerbound.....	23
4.1.1.1 Correlation between two and more signal.....	23
4.1.1.2 Power delay profile	25
4.1.1.3 Results.....	26
4.1.2 BEP Upperbound.....	28
4.2 BEP analysis for the DS-CDMA.....	28
4.2.1 BEP lowerbound.....	29
4.2.2 Multiuser effect on the BEP	30
4.2.3 Results	30
4.3 BEP comparison between MC-CDMA and DS-CDMA	32
5 Computer Simulations	33
5.1 Simulation model of the transmitter	33
5.2 Simulation model of the channel.....	34
5.3 Simulation model of the receiver	35
5.3.1 Single-user detection	35
5.3.2 Multiuser detection	37

5.4 Simulation results	37
5.5 Comparison between theoretical and simulation results	41
6 Conclusions and recommendations.....	43
References.....	45
Appendix:	49

“BER Comparison of DS-CDMA and MC-CDMA for Frequency Slective Fading Channels”

7th Tyrrhenian International Workshop on Digital Communications, 10-14 September, 1995

Introduction

Indoor wireless radio communication is becoming increasingly popular in offices, warehouses, hospitals, etc., since it offers people true mobility by freeing them from cables. Also indoor wireless radio communication reduces wiring in new buildings and provides flexibility in changing or creating various communication services in existing buildings. Until now many researches have been done in the areas of indoor wireless radio communications [1-3]. One of these areas is the multiple access scheme. Like any other wireless radio communications, indoor wireless radio communication suffers from multipath fading, which severely degrades the system performance. Multipath fading occurs when signal components, for example resulting from reflections, arrive at the receiver via two or more paths. Depending on whether the different signal components are combined constructively or destructively, the received signal will be located in a peak or a dip respectively. Two parameters that are often used to characterise the multipath channel are the root mean square (*rms*) delay spread T_m and the coherence bandwidth $(\Delta f)_c$ [4]. The delay spread T_m is a measure of the length of the impulse response of the channel. When the rms delay spread is larger than the symbol duration intersymbol interference (*ISI*) occurs. Further, the coherence bandwidth $(\Delta f)_c$ is given in [4] as (see also *Chapter 2*)

$$(\Delta f)_c \approx \frac{1}{T_m}$$

and is a measure of the correlation of fading between frequencies. If two frequencies lie within the coherence bandwidth of the channel, then they are likely to experience correlated fading. The precise definition of coherence bandwidth can differ from one reference to another [5, 6] and is subjectively determined.

In narrowband systems the corresponding narrowband signal experiences little *ISI*, since the bit duration T_b is much larger than the delay spread ($T_b \gg T_m$). However, the condition $T_b \gg T_m$ also means that the signal bandwidth is much smaller than the coherence bandwidth, thus time correlated fading is very likely to occur and the signal can totally fade.

As a solution to the above-mentioned problem, one converts the information waveform into a waveform with a much wider spectrum thus to achieve frequency diversity. The conventional DS-CDMA technique spreads the information signal by multiplying it by a pseudorandom sequence with a chip time of T_b/K_{DS} , where K_{DS} is the processing gain [7] (usually K_{DS} varies from 100 to 1000). The bandwidth of the spread signal will be K_{DS} times as large as that of the original signal. If K_{DS} is chosen to be sufficiently large, i.e. much larger than the coherence bandwidth, it is unlikely that the spread signal will totally fade. However, the delay spreads will affect the signal to a great extent and the signal will experience a considerable interchip interference, which introduces additional cross-correlation noise.

The objective of this report is to compare the performance of Multi-Carrier Code Division Multiple Access (MC-CDMA) system with that of a conventional DS-CDMA system in terms of bit error probability (BEP). It is interesting to compare the MC-CDMA system with the DS-CDMA system since many other systems have been compared to the DS-CDMA system. Further, a thorough analysis of the MC-CDMA system is necessary to come to the right choice for the implementation of a particular service in a particular environment since there are different candidates for multiple access schemes, such as TDMA [8], DS-CDMA and MC-CDMA.

The MC-CDMA scheme was proposed by Linnartz et al. in 1993 [3]. In contrary to DS-CDMA, where after signal spreading the adverse effects of the delay spread is increase as a consequent of interchip interference, the MC-CDMA spreads a signal without increasing the negative effects of the delay spread by using a number of subcarriers. In reference [3] the performance of the MC-CDMA system is studied by assuming Rayleigh fading to be Independent and Identically Distributed (IID) at each subcarrier. However, in practice, this

assumption is not correct since the subcarriers are in general highly correlated. In this report we will take the correlation between subcarriers into account by assuming an exponential Power Delay Profile (PDP). Also for the case of uncorrelated fading we discuss a uniform PDP. Further we discuss carrying out computer simulation to verify and analyse the MC-CDMA system. Receivers with RAKE structure [4] are used in both systems. It is well-known that a RAKE-receiver can combine the scattered signal power effectively and thus to produce the best performance [5].

This report is constructed as follows. In chapter 2 the general aspects of an indoor radio fading channel are discussed. One of the techniques to combat fading is diversity and here we consider the maximum ratio combining (*MRC*) technique. In chapter 3 we present system models for MC-CDMA and DS-CDMA. The transmitter, the channel and the receiver model are discussed. In chapter 4 we analyse the system performance in terms of BEP. In chapter 5 computer simulation is addressed. Conclusions and recommendations are given in chapter 6.

Multipath Fading Channel

In an indoor radio channel multipath fading is one of the most hostile propagation mechanisms and it severely degrades the system performance. The first section describes the multipath fading in detailed and the parameters which characterise the multipath channel. In the second section we discuss a diversity technique based on linear combining strategy, that is, maximum ratio combining, which can be used to combat multipath fading.

2.1 Multipath fading

In an indoor environment the signal components from different paths arrive at the receiver in different ways, often by reflections, thus multipath occurs. These components will be combined constructively or destructively depending on the phases of the components. The total received signal will be located in a peak or a dip, respectively. A useful expression that characterises the channel is the following lowpass channel equation [4]

$$c(\tau; t) = \sum_n \alpha_n(t) e^{-j2\pi f_c \tau_n(t)} \delta(\tau - \tau_n(t)) \quad (2.1)$$

where $\alpha_n(t)$ is denoted as the attenuation of the signal component at delay $\tau_n(t)$ for the n th path and f_c is the carrier frequency. Assuming the channel is Wide Sense Stationary (WSS), the autocorrelation function of $c(\tau; t)$ is given by

$$\begin{aligned}\phi_c(\tau_1, \tau_2, \Delta t) &= \frac{1}{2} E \left[c^*(\tau_1; t_1) c(\tau_2; t_2) \right] \\ &= \frac{1}{2} E \left[c^*(\tau_1; t_1) c(\tau_2; t_1 + \Delta t) \right]\end{aligned}\quad (2.2)$$

Further, if we assume the channel is *uncorrelated scattering* (US), i.e. the attenuation and the phase shift of the channel associated with path delay τ_1 is uncorrelated with those associated with the path delay τ_2 , then equation (2.2) can be written as

$$\begin{aligned}\phi_c(\tau_1, \tau_2, \Delta t) &= \phi_c(\tau_1, \tau_2, \Delta t) \delta(\tau_1 - \tau_2) \\ &= \phi_c(\tau, \Delta t) \delta(\tau - \tau_2) \quad \text{where } \tau = \tau_1\end{aligned}\quad (2.3)$$

Thus a Wide Sense Stationary Uncorrelated Scattering (WSSUS) channel can be described by using equation (2.3).

A completely analogue analysis can be done in the frequency domain by taking the Fourier transform of the time-variant multipath channel $c(\tau; t)$, thus the time-variant multipath transfer function $C(f; t)$ can be obtained,

$$C(f; t) = \int_{-\infty}^{\infty} c(\tau; t) e^{-j2\pi f\tau} d\tau \quad (2.4)$$

For a WSS channel the autocorrelation function of $C(f; t)$ can be written as

$$\phi_c(f_1, f_2, \Delta t) = \frac{1}{2} E \left[C^*(f_1; t_1) C(f_2; t_1 + \Delta t) \right] \quad (2.5)$$

Substituting equations (2.3) and (2.4) into equation (2.5) [4], we can see that uncorrelated scattering implies that the autocorrelation function $\phi_c(f_1, f_2, \Delta t)$ will only be a function of the difference of the frequencies f_1 and f_2 instead of the distinct frequencies f_1 and f_2 . Thus for a

WSSUS channel we can write $\phi_c(f_1, f_2; \Delta t)$ as $\phi_c(\Delta f; \Delta t)$, where $\Delta f = f_2 - f_1$. And $\phi_c(\Delta f; \Delta t)$ is defined as

$$\phi_c(\Delta f; \Delta t) \equiv \int_{-\infty}^{\infty} \phi_c(\tau; \Delta t) e^{-j2\pi\Delta f\tau} d\tau \quad (2.6)$$

The function $\phi_c(\Delta f; \Delta t)$ is also called the *spaced-frequency and spaced-time correlation function* of the channel. We discuss this function in more detailed in the following two subsections.

2.1.1 Delay spread and coherence bandwidth

The *multipath intensity profile*, the *delay power spectrum* or the *power delay profile* (PDP) $\phi_c(\tau)$ of the channel is defined by setting Δt equal to zero in the autocorrelation function $\phi_c(\tau; \Delta t)$. Various forms of power delay profiles have been discussed in the literature [10]: rectangular, exponential, Gaussian and triangular. In indoor environments the delay power spectra can usually be approximated by exponential functions. The range of values of τ over which $\phi_c(\tau)$ is essentially nonzero is called the *multipath spread* or *rms delay spread* and is denoted by T_m [4]. In [2] the rms delay spread T_m is defined as

$$T_m = \sqrt{E[\tau^2] - E^2[\tau]} \quad (2.7)$$

where

$$E[\tau] \equiv \frac{\sum_l \tau_l \beta_l^2}{\sum_l \beta_l^2} \quad \text{and} \quad E[\tau^2] \equiv \frac{\sum_l \tau_l^2 \beta_l^2}{\sum_l \beta_l^2} \quad (2.8)$$

where β_l is the gain of the l th path. The values of the rms delay spread depends on the size and the topography of the building under consideration. In [11] a median of the rms delay spread of 25 ns have been reported.

By taking the Fourier transform of $\phi_c(\tau)$, we obtain the spaced-frequency correlation function $\phi_c(\Delta f)$. Figure 2.1 shows the relationship between the functions $\phi_c(\tau)$ and $\phi_c(\Delta f)$, where an exponential power delay profile is assumed.

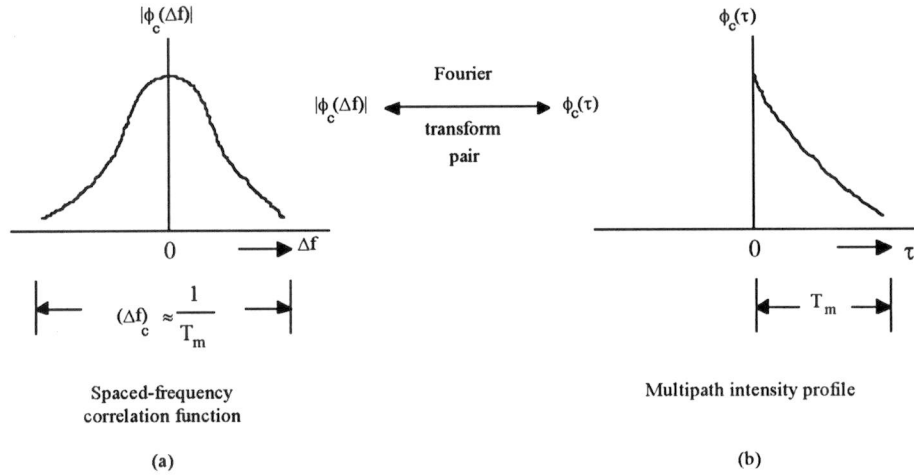


Figure 2.1 Relationship between the spaced-frequency correlation function and multipath delay profile.

The reciprocal of the multipath spread is called the *coherence bandwidth* of the channel. The coherence bandwidth is a measure of the correlation of the fading between signals of different frequencies and is given in [4] as

$$(\Delta f)_c \approx \frac{1}{T_m} \quad (2.9)$$

If the bandwidth of the transmitted signal is larger than coherence bandwidth $(\Delta f)_c$ of the channel, then the transmitted signal will undergo different gains and phase shifts across the band and be severely distorted by the channel. We say that the channel is *frequency selective*. However, if the bandwidth of the transmitted signal lies within the coherence bandwidth $(\Delta f)_c$ of the channel, the whole signal will experience the same attenuation and phase shift. In this case the channel is said to be *frequency non-selective*.

2.2.2 Doppler spread and coherence time

The *Doppler power spectrum of the channel* $S_C(\lambda)$ gives the signal intensity as a function of the Doppler frequency λ . We can obtain the function $S_C(\lambda)$ by taking the Fourier transform of the spaced-time function $\phi_c(\Delta t)$, which is defined by $\phi_c(\Delta t) \equiv \phi_c(0; \Delta t)$. The range of values of λ over which $S_C(\lambda)$ is nonzero is called the *Doppler spread* B_d of the channel. The relationship between $S_C(\lambda)$ and $\phi_c(\Delta t)$ is shown in figure 2.2, where a Gaussian Doppler power spectrum is assumed.

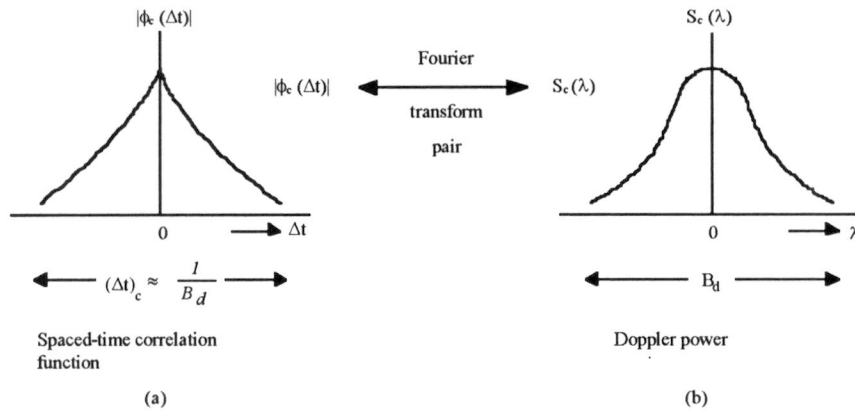


Figure 2.2 Relationship between the spaced-time correlation function and the Doppler power spectrum.

The reciprocal of the Doppler spread is a measure of the *coherence time* of the channel, i.e.

$$(\Delta t)_c \approx \frac{1}{B_d} \quad (2.10)$$

where $(\Delta t)_c$ is the coherence time. A slowly changing channel has a large coherence time, which correspond to a small Doppler spread.

2.2 Diversity techniques

Diversity techniques can be used to combat mutipath fading. There are different kinds of

diversity techniques [9]: frequency diversity, time diversity, space diversity, polarisation diversity etc. In this report a diversity technique base on linear combining is considered: Maximum Ratio Combining (*MRC*). One type of receiver which uses this technique is called the RAKE-receiver. The RAKE-receiver combines the scattered power of the signals such that it produces an optimum signal in the sense of BEP performance. The time-domain RAKE-receiver uses time diversity while the frequency domain RAKE-receiver uses frequency diversity.

MC-CDMA and DS-CDMA Systems

DS-CDMA is a familiar protocol [12-15]. On the contrary MC-CDMA, which is based on spread spectrum technique, is a fairly new protocol and was proposed by Linnartz et al. in 1993 [3]. Unlike the conventional DS-CDMA technique, where spreading of a signal is achieved by multiplying the information signal with a pseudorandom sequence with a chip time of T_b/K_{DS} , spreading of a signal in MC-CDMA system is achieved by adding up the coded narrowband signals. The main advantage of MC-CDMA scheme over the conventional DS-CDMA scheme, where negative effects of time spreads are increased because of interchip interference, is that negative effects of time spreads do not increase. However one of the disadvantages is that the complexity and the costs of the transmitter and receiver will increase linearly with the number of narrowband signals in the spread signal.

Throughout the report only the performance of the downlink (from base station to mobile) is considered. In this chapter we present system models for MC-CDMA and DS-CDMA in order to evaluate and compare their performances. We consider frequency selective slow Rayleigh fading channels. To make a fair comparison we assume the same kinds of PDPs. An

for the case of heavy frequency selective fading. In the first section we consider the MC-CDMA system and in the second section the DS-CDMA system. In the last section the design of the systems and their parameters are discussed.

3.1 MC-CDMA system

In this section we present the MC-CDMA system model. The MC-CDMA system uses the *Walsh-Hadamard (WH)* code, which is a member of the family of orthogonal codes, to achieve multiple access. Each user is assigned to a particular WH code sequence. The transmitter, channel and receiver models are considered.

3.1.1 Base station model

The transmitter model is shown in figure 3.1, where a each data symbol is replicated into K_{MC} parallel copies. Each copy is multiplied by a chip of a PN code of length K_{MC} and then BPSK modulated with a number of subcarriers with a space of Δf among each subcarrier.

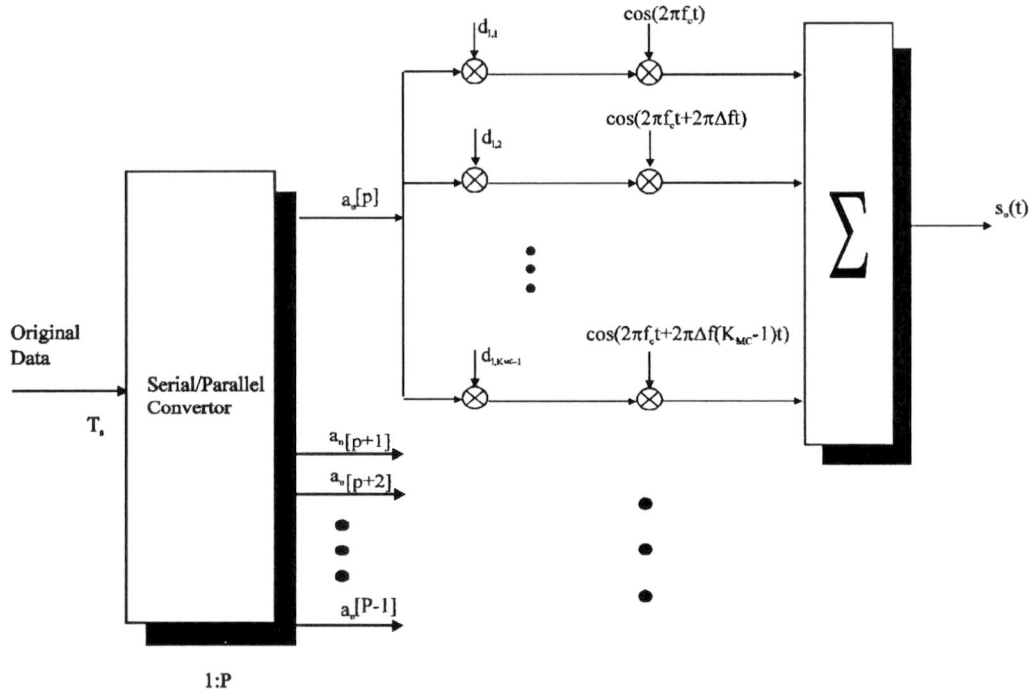


Figure 3.1 Transmitter model the MC-CDMA.

At the end of the transmitter all these signals with different subcarriers will be added up and transmitted. Thus the transmitted signal of user n can be written as

$$s_n(t) = \sum_{p=0}^{\infty} \sum_{k=0}^{K_{MC}-1} a_n[p] d_{n,k} \cos(2\pi f_c t + 2\pi \Delta f k t) p_{T_b}(t - pT_b) \quad (3.1)$$

where $a_n[p]$ is the p th bit of the data sequence and $\{d_{n,k}\}$ is the Walsh-Hadamard code sequence of the n th user, and $P_{T_b}(t)$ is an unit pulse that is non-zero in the interval of 0 and T_b . The frequency separation $\Delta f = 1/T_s$, where T_s is the symbol duration.

In the base station all the signals of different users are added up and transmitted. Thus the transmitted signal of the base station will be

$$s(t) = \sum_{l=1}^L s_l(t) \quad (3.2)$$

where L is the number of active users in the system. The power spectrum of the signal $s(t)$ is shown in figure 3.2.

Power spectrum of the MC-CDMA signal

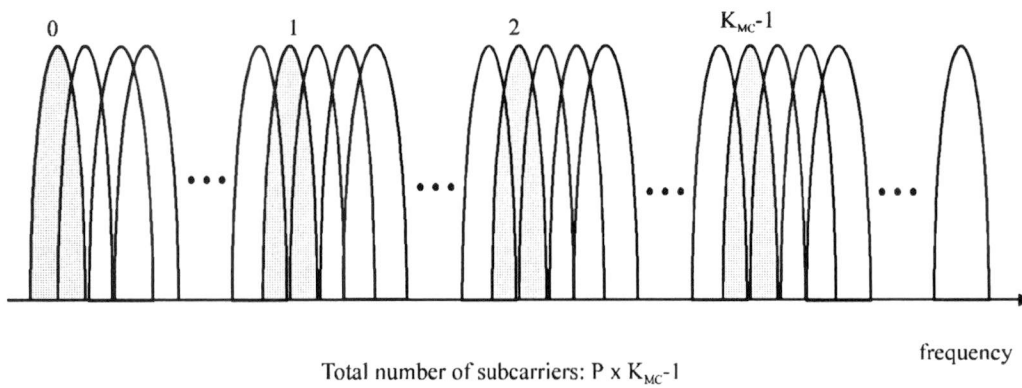


Figure 3.2 Power spectrum of the MC-CDMA signal.

3.1.2 Channel model

We consider *frequency selective slow Rayleigh fading* channels. Since the MC-CDMA signal is best described in the frequency domain, we use the transfer function of the continuous-time fading channel equation to describe the channel. This transfer function is given as

$$H(f_c + \Delta f k) = R_k e^{j\theta_k} \quad (3.3)$$

where R_k and ϕ_k are the random variables of the amplitudes and phases respectively. R_k is assumed to be a Rayleigh random variable and its probability density function (pdf) is given as [15]

$$f_{R_k}(r) = \frac{r}{\sigma^2} \exp\left[-\frac{r^2}{2\sigma^2}\right] \quad (3.4)$$

where σ^2 is the variance of the random amplitude and is determined by the power delay profile. The Rayleigh fading mechanism is illustrated in figure 3.3. As can be seen the specular or *line-of-sight (LOS)* component is assumed to be absent.

Rayleigh fading

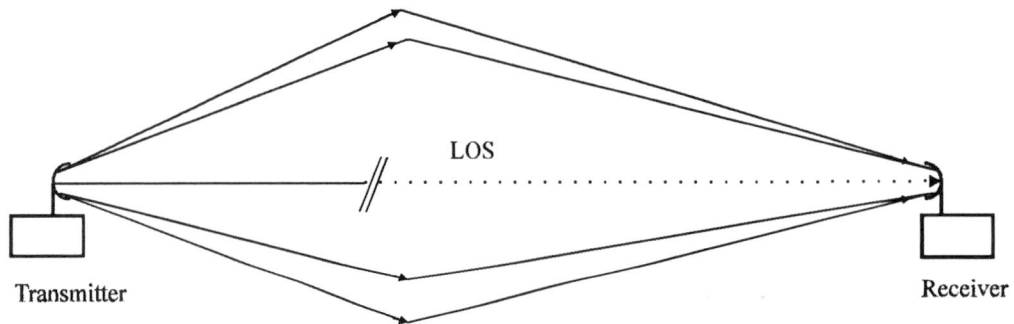


Figure 3.3 Illustration of Rayleigh fading channels.

The received signal of the p th bit can be written as

$$r(t) = \sum_{l=1}^L \sum_{k=0}^{K_{MC}-1} R_k d_{l,k} a_l[p] \cos(2\pi f_c t + 2\pi \Delta f k t + \phi_k) + n(t) \quad (3.5)$$

where $n(t)$ is the AWGN with one-sided power spectral density of N_0 .

3.1.3 Receiver model

The receiver model of the user n is shown in figure 3.4, where we assume a perfect carrier synchronisation. First the received signal $r(t)$ is coherently demodulated and then multiplied by $d_{n,k} G_k$, where G_k is the gain.

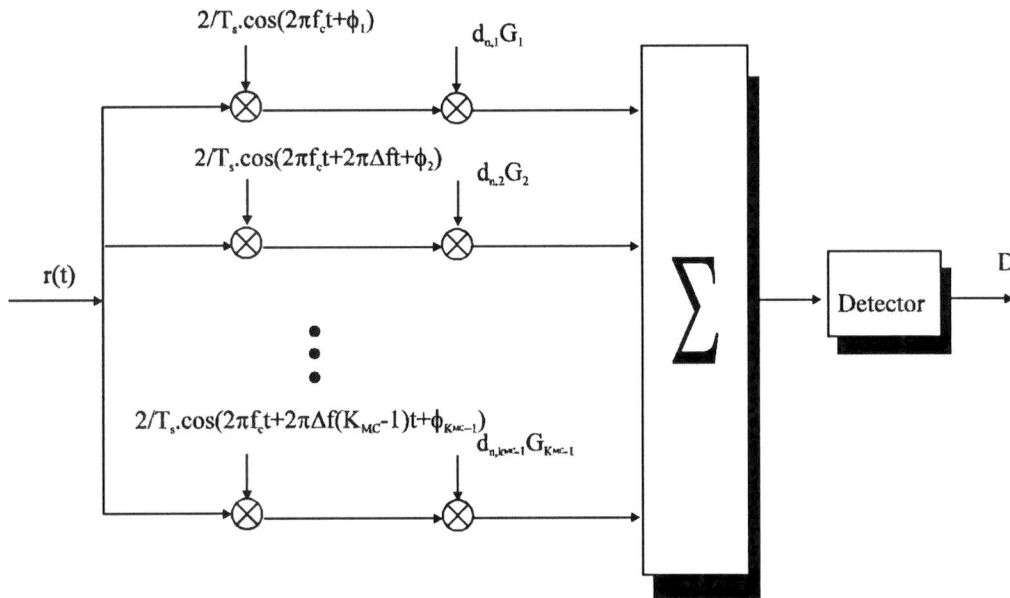


Figure 3.4 Receiver model of the user n in the MC-CDMA system.

The decision variable D on the p th bit can be written as

$$\begin{aligned} D &= \sum_{k=1}^{K_{MC}-1} \left\{ \sum_{l=1}^L R_k d_{l,k} a_l[p] \times G_k \right\} + \sum_{k=0}^{K_{MC}-1} \int_0^{T_b} n_k(t) G_k \cos(2\pi f_c t + 2\pi \Delta f k t + \phi_k) dt \\ &= \sum_{k=1}^N G_k R_k a_n[p] + \sum_{k=0}^{K_{MC}-1} \sum_{\substack{l=1 \\ l \neq n}}^L R_k G_k a_l[p] + \eta \end{aligned} \quad (3.6)$$

The first term in the summation is due to the desired signal, the second term and the third terms are the multiuser interference and noise respectively. A frequency domain RAKE-receiver is realised by choosing the gain G_k as R_k . When choosing the gain G_k as $1/R_k$, the orthogonality of the signal can be perfectly be restored.

3.2 DS-CDMA system

In this section we present a DS-CDMA system model. Figure 3.5 shows the block diagram of the DS-CDMA system with RAKE-receiver. The binary information sequence $b(t)$ is modulated twice, once by a PN sequence and once by a conventional modulator, such as BPSK or QPSK modulator. The modulator and demodulator are the basic elements in the system. When a signal passes through a frequency selective channel, different copies of the signals with different delays will reach the receiver. The RAKE-receiver attempts to resolve the multiple-path components and appropriately combine them for time diversity advantages [10].

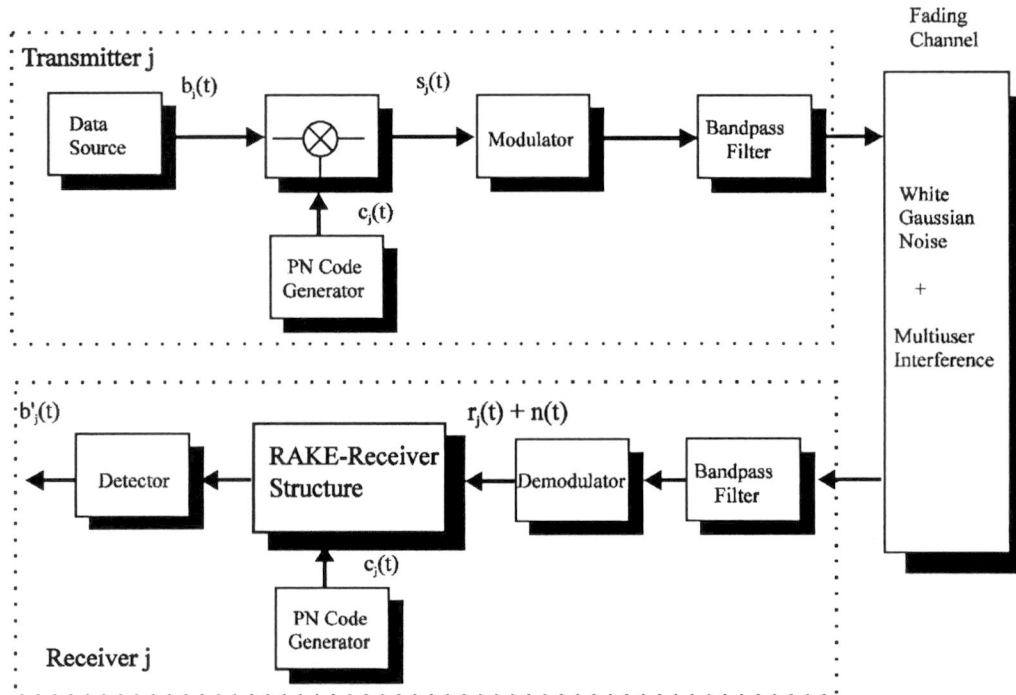


Figure 3.5 Block diagram of DS-CDMA system.

3.2.1 Base station model

The basic idea of the DS-CDMA scheme is to modulate the information signal with a wideband noise-like (PN) code sequence. This process is shown in figure 3.6. Demodulation is done by multiplying the received signal by the same PN code. BPSK is employed throughout the report. The complex-lowpass expression of the transmitted signal is of the form

$$s_j(t) = \sum_{k=1}^{K_{DS}} b_j(k) c_j(k) u(t - kT_c) \quad (3.7)$$

The transmitted signal of the base station will be the sum of signals of different users $s(t)$ and can be written as follows

$$s(t) = \sum_{j=1}^J s_j(t) \quad (3.8)$$

where J is the total number of active users in the system.

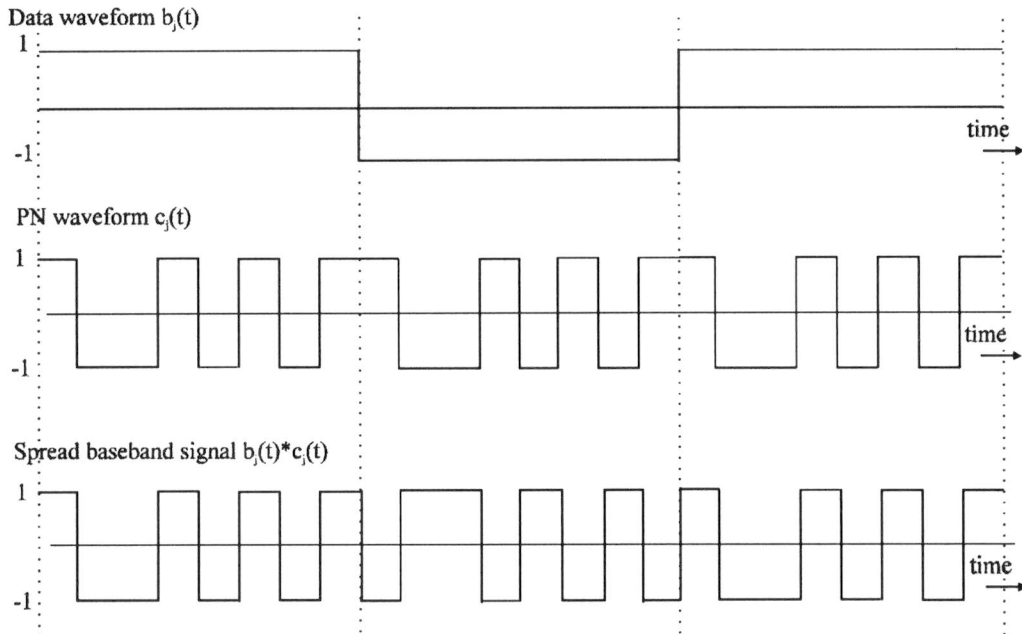


Figure 3.6 Multiplication of the information signal with a PN sequence.

3.2.2 Channel model

As in the case of the MC-CDMA system, the same *WSSUS* channel with frequency selective slow Rayleigh fading is considered. The complex equivalent lowpass time-variant impulse response can be written as [4]

$$h(\tau, t) = \sum_{l=1}^L g_l(t) \delta(\tau - \tau_l) \quad (3.9)$$

where t and τ are the time and the time delay, respectively, L is the number of resolvable paths, $g_l(t)$ is the complex envelope of the signal received on the l -th path which is a complex Gaussian random process with zero mean and variance σ_l^2 , which is determined by the power delay profile, and τ_l is the propagation delay for the l -th path. The factor $g_l(t)$ is given as

$$g_l(t) = G_l \cdot e^{j\theta_l(t)} \quad (3.10)$$

where G_l is a Rayleigh random variable with variance σ_l^2 and $\theta_l(t)$ is a random variable uniformly distributed in $[0, 2\pi)$. Further the number of the resolvable paths is given according to the following expression

$$L = \left\lfloor \frac{T_m}{T_c} \right\rfloor + 1 \quad (3.11)$$

where $\lfloor x \rfloor$ is the largest integer less than or equal to x . This equation is based on the time resolution of direct sequence spread spectrum signal, which is equal to the chip duration T_c . The received signal will be of the form

$$r(t) = \sum_{j=1}^J r_j(t) + n(t) \quad (3.12)$$

where $n(t)$ is the AWGN with one-sided power spectral density N_o and $r_j(t)$ is given as

$$r_j(t) = \sum_{l=1}^L s_j(t) * h(\tau, t) \quad (3.13)$$

where $*$ denotes the convolution.

3.2.3 Receiver model

Figure 3.7 shows a model of the time domain RAKE-receiver for the DS-CDMA system. In each arm the received signal is delayed by τ_l and despread by code j . After the signal is despread it will be multiplied by the complex conjugate of the path gains. Finally, different copies of the signal will be added up and go to the detector.

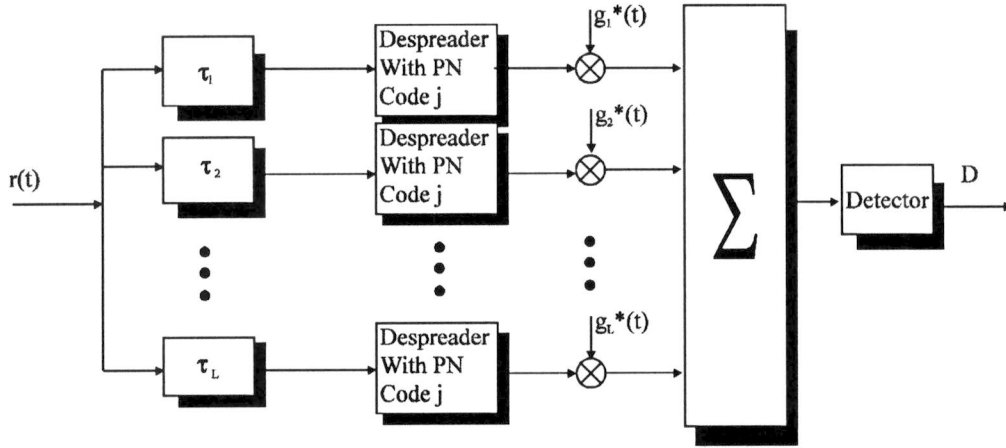


Figure 3.7 Time-domain RAKE-receiver.

The decision variable D , which is the output of the detector, can be written as

$$D = \sum_{l=1}^L R_l^2 + \sum_{l=1}^L R_l N_k \quad (3.14)$$

where N_k is given as

$$N_k = e^{j\theta_k} \int_0^{T_b} n(t) dt \quad (3.15)$$

3.3 Design of the systems

In practice spreading and despreading of the MC-CDMA signal is done by the Discrete Fourier Transform (DFT). The number of subcarriers is thus determined by N-point FFT. In [17] it is shown that there exists an optimum number of N to minimise the BEP. This can be seen as follows: as the number of subcarriers increases the transmission performance becomes more sensitive to the time selectivity because the wider symbol duration is less robust to the random FM noise, but as the number of subcarriers decreases the transmission performance becomes poor because the wider power spectrum of each subcarrier is less robust to the frequency selectivity. Also there exists an optimum guard duration Δ to minimise the BEP: as Δ increases the more power will be lost, but as Δ decreases the transmission performance will degrade because of increasing sensitivity to frequency-selectivity.

The MC-CDMA system with 1024 subcarriers, when the processing gain is 32, will use 32 subcarriers for each data symbol. By choosing Δ as 100 ns we can minimise the BEP (see Appendix A). Here the data rate is chosen as 3 Mps, so the total bandwidth will be 96 MHz. As known the bandwidth of DS-CDMA system, when using the same processing gain, will be twice of the MC-CDMA system.

The following system parameters are used:

	MC-CDMA	DS-CDMA
Code Type	Walsh-Hadamard codes	Gold codes
Processing Gain	32	31
Bit Rate	3 Mps	3 Mps
Bandwidth	96 MHz	186 MHz
RMS delay spread	20 ns	20 ns

BEP Performance Analysis

In this chapter the BEP performances of MC-CDMA and DS-CDMA systems are analysed. The concept of analysis is based on the characteristic function method for the quadratic form of Gaussian random variables [5]. We consider the best performance, identical to BEP lowerbound, and compare the BEP between these systems. In the first section we consider the BEP analysis for the MC-CDMA system and in the second section the BEP analysis for the DS-CDMA system.

4.1 BEP analysis for the MC-CDMA system

First we analyse the BEP lowerbound, which is identical to the BEP for the case of a single active user with a frequency domain RAKE-receiver. Also the BEP upperbound is considered. Unfortunately it has no closed form, so we have to resort to computer simulation, which is reported in the following chapter.

4.1.1 BEP lowerbound

We can obtain the BEP lowerbound when we assume that there is only a single active user in the system and the combination of the received signal at each subcarrier is based on MRC. In

this case the gain G_k is chosen as R_k^* . Assuming $+1$ is transmitted, equation (3.6) becomes

$$D = \sum_{k=0}^{K_{MC}-1} R_k^2 + \eta \quad (4.1)$$

where η is given as

$$\eta = \sum_{k=0}^{K_{MC}-1} \int_0^{T_b} n y(t) R_k^* \cos(2\pi f_c t + 2\pi \Delta f k t + \phi_k) dt \quad (4.2)$$

Thus the BEP lowerbound of the MC-CDMA system can be written as [4]

$$\begin{aligned} BEP_{MC} = & \int_{-\infty}^{+\infty} \int_{-\infty}^{+\infty} \dots \int_{-\infty}^{+\infty} \frac{1}{2} \operatorname{erfc} \left[\sqrt{\frac{(X_0^2 + Y_0^2) + (X_1^2 + Y_1^2) + \dots + (X_{K_{MC}-1}^2 + Y_{K_{MC}-1}^2)}{2\sigma_n^2}} \right] \\ & \times p(X_0, Y_0, X_1, Y_1, \dots, X_{K_{MC}-1}, Y_{K_{MC}-1}) dX_0 dY_0 dX_1 dY_1 \dots dX_{K_{MC}-1} dY_{K_{MC}-1} \end{aligned} \quad (4.3)$$

where X_k and Y_k are the inphase and quadrature phase components of R_k , respectively, and which are independent Gaussian random variables with zero mean and variance σ_n^2 and $p(X_0, Y_0, X_1, Y_1, \dots, X_{K_{MC}-1}, Y_{K_{MC}-1})$ is the joint pdf of Gaussian random variables and is given as

$$p(X_0, Y_0, X_1, Y_1, \dots, X_{K_{MC}-1}, Y_{K_{MC}-1}) = \frac{1}{(2\pi)^{K_{MC}} \sqrt{\det(M)}} \exp \left[-\frac{1}{2} H M^{-1} H^T \right] \quad (4.4)$$

where M^{-1} is the inverse of the covariance matrix M and M and H are defined as follows

$$\begin{aligned} M &= \langle H^T \cdot H \rangle \\ H &= (X_0, X_1, \dots, X_{K_{MC}-1}, Y_0, Y_1, \dots, Y_{K_{MC}-1}) \end{aligned} \quad (4.5)$$

where $\langle x \rangle$ denotes the average of x . Using the approximation $\operatorname{erfc}(x) \approx \exp(-x^2)/2$, which is based on the fact that there is a difference of 3 dB in BEP between DBPSK and CBPSK [4], the above equation can be simplified as

$$\begin{aligned}
 BEP_{MC} \approx & \int_{-\infty}^{+\infty} \int_{-\infty}^{+\infty} \dots \int_{-\infty}^{+\infty} \frac{1}{4} \exp \left[-\frac{(X_0^2 + Y_0^2) + (X_1^2 + Y_1^2) + \dots + (X_{K_{MC}-1}^2 + Y_{K_{MC}-1}^2)}{2\sigma_n^2} \right] \\
 & \times p(X_0, Y_0, X_1, Y_1, \dots, X_{K_{MC}-1}, Y_{K_{MC}-1}) dX_0 dY_0 dX_1 dY_1 \dots dX_{K_{MC}-1} dY_{K_{MC}-1}
 \end{aligned} \quad (4.6)$$

This equation is equivalent to the following characteristic function with $ju = -1/2\sigma_n^2$

$$\begin{aligned}
 BEP_{MC} = & \int_{-\infty}^{+\infty} \int_{-\infty}^{+\infty} \dots \int_{-\infty}^{+\infty} \frac{1}{4} \exp \left[ju(X_0^2 + Y_0^2) + (X_1^2 + Y_1^2) + \dots + (X_{K_{MC}-1}^2 + Y_{K_{MC}-1}^2) \right] \\
 & \times p(X_0, Y_0, X_1, Y_1, \dots, X_{K_{MC}-1}, Y_{K_{MC}-1}) dX_0 dY_0 dX_1 dY_1 \dots dX_{K_{MC}-1} dY_{K_{MC}-1} \\
 = & \frac{1}{4} C(ju) \Big|_{ju = -\frac{1}{2\sigma_n^2}}
 \end{aligned} \quad (4.7)$$

For Rayleigh fading channels $\langle H \rangle$ is equal to a zero vector. Equation (4.7) can be written as [10]

$$BEP_{MC} = \frac{1}{4} \times \frac{1}{\sqrt{\det(I - 2juMQ)}} \Big|_{ju = -\frac{1}{2\sigma_n^2}} = \frac{1}{4} \prod_{k=0}^{K_{MC}-1} \frac{1}{1 + \lambda_k \gamma} \quad (4.8)$$

where λ_k 's are the eigenvalues of the covariance matrix M , γ is defined as the ratio between E_b and N_0 , and Q is defined as follows

$$\begin{aligned}
 HQH^T = & (X_0^2 + Y_0^2) + (X_1^2 + Y_1^2) + \dots + (X_{K_{MC}-1}^2 + Y_{K_{MC}-1}^2) \\
 Q = & \begin{bmatrix} 1 & \dots & 0 \\ 0 & \ddots & 0 \\ 0 & \dots & 1 \end{bmatrix}
 \end{aligned} \quad (4.9)$$

4.1.1.1 Correlation between two and more signals

Let us consider a case for two complex Gaussian random variables $z_1 = x_1 + jy_1$ and $z_2 = x_2 + jy_2$

and let ρ_{12} be the complex correlation coefficient of these variables, then the correlation coefficient between these two variables is given by

$$\rho_{12} = \rho_{r,12} + j\rho_{i,12} = \frac{1}{2} \langle z_1^* \cdot z_2 \rangle \quad (4.10)$$

where ρ_r and ρ_i are the real and imaginary parts of ρ respectively. When using the relations

$$\begin{aligned} \langle x_1 \cdot x_2 \rangle &= \langle y_1 \cdot y_2 \rangle \\ \langle x_1 \cdot y_2 \rangle &= -\langle y_1 \cdot x_2 \rangle \end{aligned} \quad (4.11)$$

we can get the following relations

$$\begin{aligned} \langle x_1 \cdot x_2 \rangle &= \sigma^2 \rho_{r,12} \\ \langle y_1 \cdot y_2 \rangle &= \sigma^2 \rho_{r,12} \\ \langle x_1 \cdot y_2 \rangle &= \sigma^2 \rho_{i,12} \\ \langle y_1 \cdot x_2 \rangle &= -\sigma^2 \rho_{i,12} \end{aligned} \quad (4.12)$$

In this case the covariance matrix M of $H=[x_1, x_2, y_1, y_2]$ is

$$M = \sigma^2 \begin{bmatrix} 1 & \rho_{r,12} & 0 & \rho_{i,12} \\ \rho_{r,12} & 1 & -\rho_{i,12} & 0 \\ 0 & -\rho_{i,12} & 1 & \rho_{r,12} \\ \rho_{i,12} & 0 & \rho_{r,12} & 1 \end{bmatrix} \quad (4.13)$$

Consequently when using K_{MC} subcarriers we have the following $2 \times K_{MC}$ covariance matrix

$$\begin{aligned}
M &= \begin{bmatrix} \langle x_1 \cdot x_1 \rangle & \langle x_1 \cdot x_2 \rangle & \dots & \langle x_1 \cdot x_N \rangle & \langle x_1 \cdot y_1 \rangle & \langle x_1 \cdot y_2 \rangle & \dots & \langle x_1 \cdot y_N \rangle \\ \langle x_2 \cdot x_1 \rangle & \langle x_2 \cdot x_2 \rangle & \dots & \langle x_2 \cdot x_N \rangle & \langle x_2 \cdot y_1 \rangle & \langle x_2 \cdot y_2 \rangle & \dots & \langle x_2 \cdot y_N \rangle \\ \vdots & & \ddots & & \vdots & & & \vdots \\ \langle x_N \cdot x_1 \rangle & \langle x_N \cdot x_2 \rangle & \dots & \langle x_N \cdot x_N \rangle & \langle x_N \cdot y_1 \rangle & \langle x_N \cdot y_2 \rangle & \dots & \langle x_N \cdot y_N \rangle \\ \langle y_1 \cdot x_1 \rangle & \langle y_1 \cdot x_2 \rangle & \dots & \langle y_1 \cdot x_N \rangle & \langle y_1 \cdot y_1 \rangle & \langle y_1 \cdot y_2 \rangle & \dots & \langle y_1 \cdot y_N \rangle \\ \langle y_2 \cdot x_1 \rangle & \langle y_2 \cdot x_2 \rangle & \dots & \langle y_2 \cdot x_N \rangle & \langle y_2 \cdot y_1 \rangle & \langle y_2 \cdot y_2 \rangle & \dots & \langle y_2 \cdot y_N \rangle \\ \vdots & & \ddots & & \vdots & & & \vdots \\ \langle y_N \cdot x_1 \rangle & \langle y_N \cdot x_2 \rangle & \dots & \langle y_N \cdot x_N \rangle & \langle y_N \cdot y_1 \rangle & \langle y_N \cdot y_2 \rangle & \dots & \langle y_N \cdot y_N \rangle \end{bmatrix} \\
&= \sigma^2 \begin{bmatrix} 1 & \rho_{r,12} & \dots & \rho_{r,1N} & 0 & \rho_{i,12} & \dots & \rho_{i,1N} \\ \rho_{r,12} & 1 & \dots & \rho_{r,2N} & -\rho_{i,12} & 0 & \dots & \rho_{i,2N} \\ \vdots & & \ddots & & \vdots & & \ddots & \vdots \\ \rho_{r,1N} & \rho_{r,2N} & \dots & 1 & -\rho_{i,1N} & -\rho_{i,2N} & \dots & 0 \\ 0 & -\rho_{i,12} & \dots & -\rho_{i,1N} & 1 & \rho_{r,12} & \dots & \rho_{r,1N} \\ \rho_{i,12} & 0 & \dots & -\rho_{i,2N} & \rho_{r,12} & 1 & \dots & \rho_{r,2N} \\ \vdots & & \ddots & & \vdots & & \ddots & \vdots \\ \rho_{i,1N} & \rho_{i,2N} & \dots & 0 & \rho_{r,1N} & \rho_{r,2N} & \dots & 1 \end{bmatrix} \quad (4.14)
\end{aligned}$$

4.1.1.2 Power delay profile

We can calculate the complex correlation coefficients ρ by using the spaced-frequency correlation function (see chapter 2). We can easily take into account different kinds of power delay profiles by considering their corresponding frequency correlation functions. For an exponential power delay profile the spaced-frequency correlation function can be written as

$$\phi_c(\tau) = \frac{\sigma^2}{\tau_{rms}} e^{-\frac{\tau}{\tau_{rms}}} \quad \xleftrightarrow{F} \quad \phi_C(\Delta f) = \frac{\sigma^2}{1 + j2\pi\tau_{rms}(\Delta f)} \quad (4.15)$$

where Δf is the frequency separation between the two signals. For a uniform power delay profile the following frequency correlation function is used

$$\phi_c(\tau) = \sigma^2 \quad \xleftrightarrow{F} \quad \phi_C(\Delta f) = \sigma^2 \delta(\Delta f) \quad (4.16)$$

this means that the covariance matrix is a diagonal matrix. Clearly, this kind of PDP does not exist in reality since an infinite signal energy is needed. However, it is interesting to look at it because two arbitrary signals will always be completely uncorrelated.

4.1.1.3 Results

Figure 4.1 shows the BEP lowerbound of the MC-CDMA system as a function of E_b/N_0 for the exponential power delay profiles with different rms delays and a uniform power delay profile. We can see that the BEP improves with increase of delays. This is because the multiple signals, which arrive at the receiver, have less correlation among subcarriers and MRC can take full advantage of frequency diversities. When the subcarriers are completely uncorrelated, which is the case in respect to the uniform PDP, the BEP will be the best, as can be seen from the figure.

Figure 4.2 shows the BEP lowerbound of the MC-CDMA system as a function of E_b/N_0 for different bitrates. The bandwidth remains constant and is taken as 96 MHz. As expected, the BEP decreases with a decrease in the data rate. Also, it can be seen that a further decrease in the data rate of less than 6 Mps to improve the BEP does not make sense, since the BEP of 3 Mps and 6 Mps does not differ much.

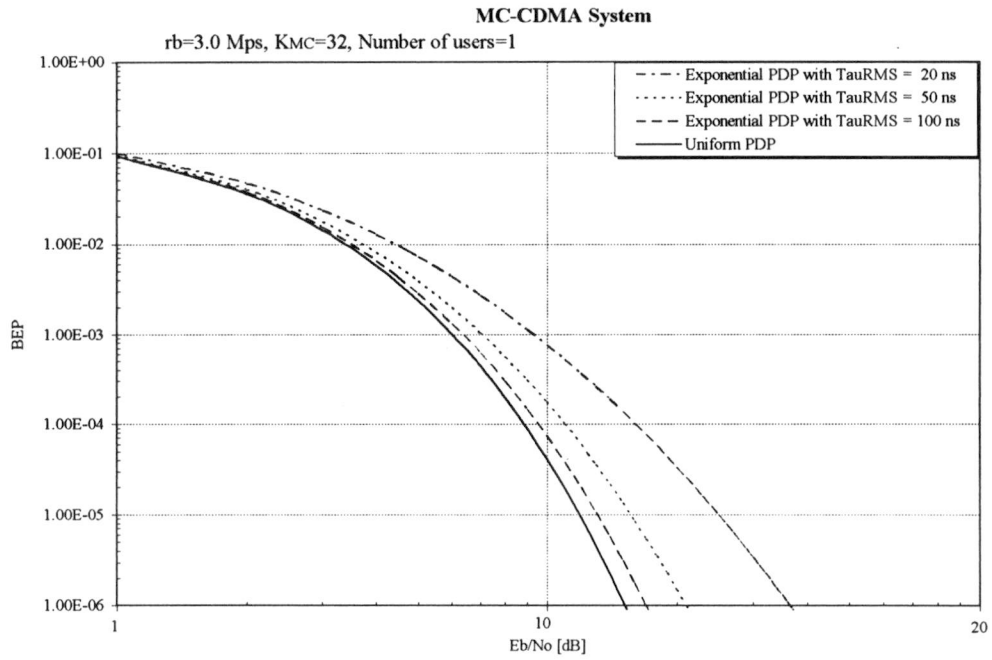


Figure 4.1 BEP versus E_b/N_0 for uniform and exponential PDPs with different RMS delays.

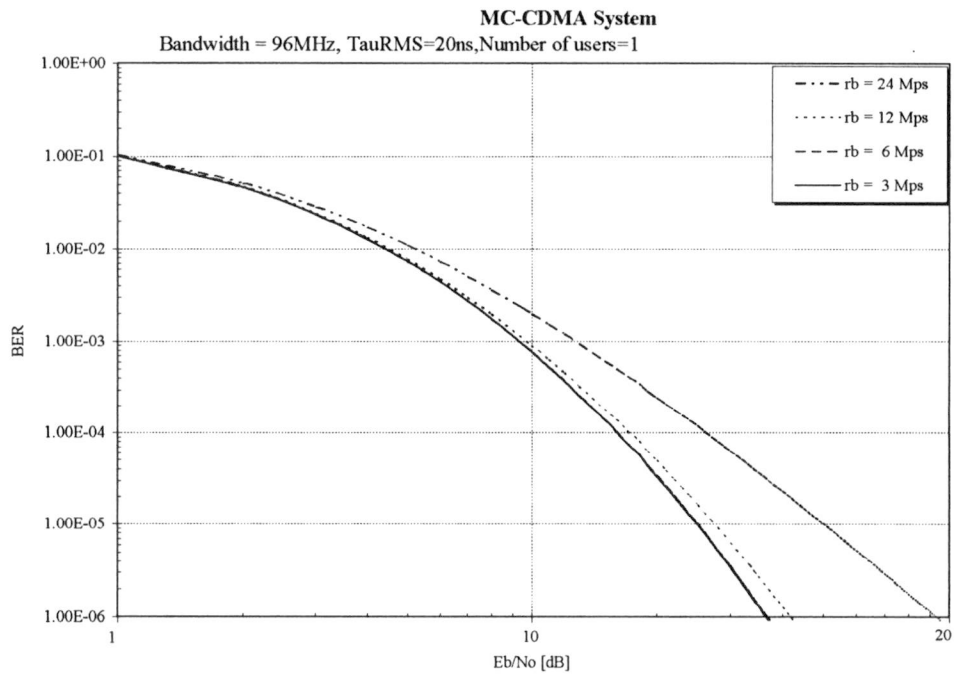


Figure 4.2 BEP versus E_b/N_0 for MC-CDMA system with different data rates. Exponential PDP is assumed.

4.1.2 BEP upperbound

When we choose the gain $G_k = I/R_k$ we can perfectly reject the interference of other active users since the orthogonality of the WH codes is recovered. But by doing so the noise will be amplified for the weaker received subcarriers. This give us the BEP upperbound. In this case, the decision variable D can be written as

$$D = \sum_{k=0}^{K_{MC}-1} 1 + \eta \quad (4.17)$$

where η is given as

$$\eta = \sum_{k=0}^{K_{MC}-1} \int_0^{T_b} \frac{n(t) \cos(2\pi f_c t + 2\pi \Delta f k t + \phi_k)}{R_k} dt \quad (4.18)$$

The corresponding BEP is

$$BEP_{MC} = \int_{-\infty}^{+\infty} \int_{-\infty}^{+\infty} \dots \int_{-\infty}^{+\infty} \frac{1}{2} \operatorname{erfc} \left[\sqrt{\frac{1}{2\sigma_n^2} \frac{K_{MC}^2}{\frac{1}{(X_0^2 + Y_0^2)} + \frac{1}{(X_1^2 + Y_1^2)} + \dots + \frac{1}{(X_{K_{MC}-1}^2 + Y_{K_{MC}-1}^2)}}} \right] \times p(X_0, Y_0, X_1, Y_1, \dots, X_{K_{MC}-1}, Y_{K_{MC}-1}) dX_0 dY_0 dX_1 dY_1 \dots dX_{K_{MC}-1} dY_{K_{MC}-1} \quad (4.19)$$

Unfortunately, the above equation can not be simplified in any close form neither can it be simplified in a quadratic form. Thus we have to resort to computer simulation, which is discussed in the next chapter.

4.2 BEP analysis for the DS-CDMA system

In this section the BEP lowerbound for the DS-CDMA system with the time-domain RAKE-receiver is analysed. Also the multiuser interference is taken into account in the BEP analysis based on a Gaussian approximation.

4.2.1 BEP lowerbound

Using equation (3.14) the BEP of the DS-CDMA system is given by [4]

$$BEP_{DS} = \int \int_{-\infty}^{+\infty} \dots \int \frac{1}{2} \operatorname{erfc} \left[\sqrt{\frac{(X_1^2 + Y_1^2) + (X_2^2 + Y_2^2) + \dots + (X_L^2 + Y_L^2)}{2\sigma_n^2}} \right] p(X_1, Y_1; X_2, Y_2; \dots X_L, Y_L) dX_1 dY_1 dX_2 dY_2 \dots dX_L dY_L \quad (4.20)$$

where $p(X_1, Y_1; X_2, Y_2; \dots X_L, Y_L)$ is $2L$ dimensional independent joint Gaussian pdf as given in equation (4.4).

$$p(X_1, Y_1; X_2, Y_2; \dots X_L, Y_L) = \frac{1}{(2\pi)^L \sqrt{\det(M)}} \exp \left[-\frac{1}{2} H M^{-1} H^T \right] \quad (4.21)$$

For the DS-CDMA system independent fading characteristic can be assumed in the received signals at different paths. Thus M is a diagonal matrix and H and M are respectively given by

$$H = (X_1, X_2, \dots, X_L, Y_1, Y_2, \dots, Y_L)$$

$$M = \begin{bmatrix} \sigma_1^2 & 0 & \dots & 0 \\ 0 & \sigma_2^2 & & \\ \vdots & & \ddots & \vdots \\ 0 & \dots & 0 & \sigma_L^2 \\ & & \sigma_1^2 & \\ \vdots & & & \ddots & 0 \\ 0 & \dots & & 0 & \sigma_L^2 \end{bmatrix} \quad (4.22)$$

The diversity order depends on the number of the arms of RAKE receiver. Because of the hardware complexity in practice, the RAKE-receiver is mostly of the order one, two or three. The number of resolvable paths L is determined according to equation (3.11).

4.2.2 Multiuser effect on the BEP

Using the expressions in [10] we can easily take the multiuser effect on the BEP into account. When assuming that the sum of the interfering signals are Gaussian distributed, the variance of the cross-correlation by using Gold codes is

$$\sigma_{K_{DS}}^2 = \frac{2(J-1)}{3K_{DS}} E_b \quad (4.23)$$

where J is the number of active users. The Gaussian assumption is correct when the numbers of these signals are large i.e. $JK \gg 1$. Then the total noise σ_n^2 will be

$$\sigma_n^2 = N_o + \sigma_{K_{DS}}^2 = N_o + \frac{2(J-1)}{3K_{DS}} E_b \quad (4.24)$$

Thus the total noise is the sum of the thermal noise and the multiuser interference.

4.2.3 Results

The BEP lowerbounds of the DS-CDMA system, when using the time-domain RAKE-receiver, for different τ_{RMS} is shown in figure 4.3. When the rms delay increases, the BEP will decrease, as in the case of the MC-CDMA system. A bigger τ_{RMS} means that we can use a higher time resolution and thus increase the number of arms in the RAKE-receiver.

Figure 4.4. shows the BEP versus E_b/N_o for DS-CDMA system with different numbers of users. As expected, the BEP increases with the increasing number of simultaneous users.

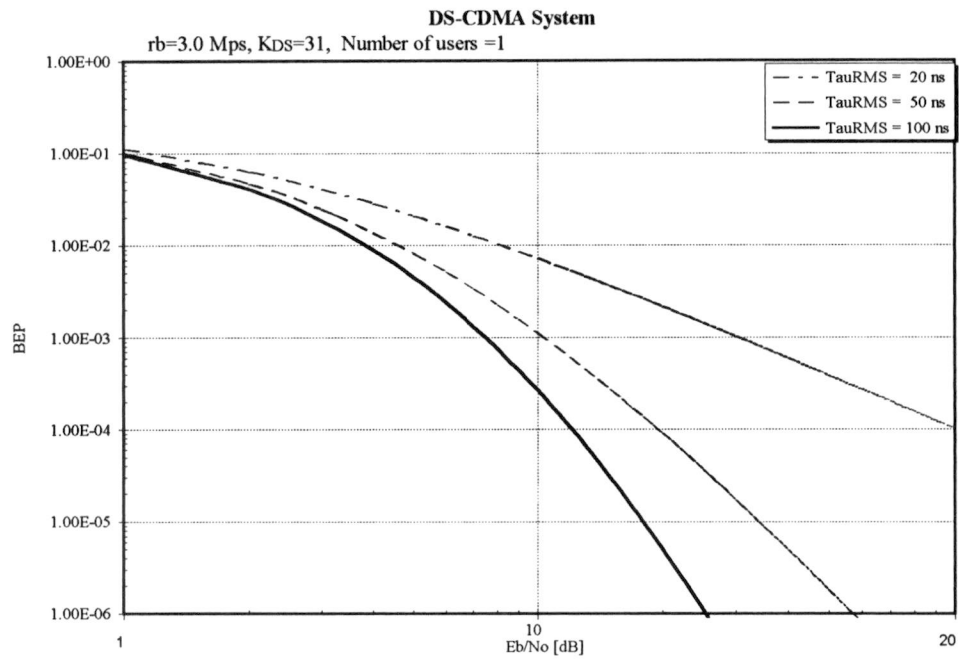


Figure 4.3 BEP versus E_b/N_0 for a DS-CDMA with different RMS delays.

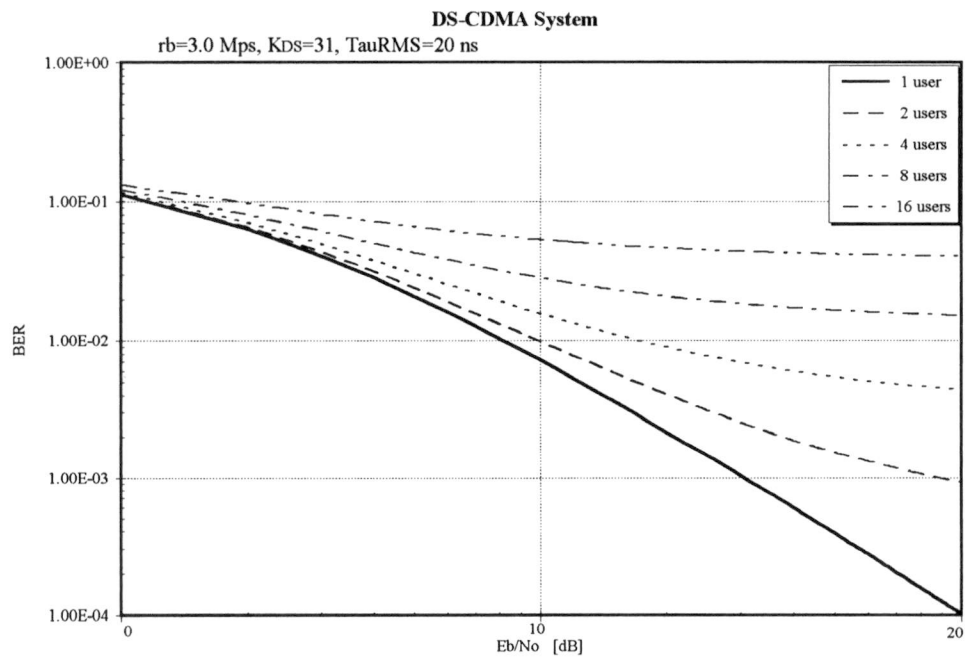


Figure 4.4 BEP versus E_b/N_0 for a DS-CDMA system with different users.

4.3 BEP comparison between MC-CDMA and DS-CDMA

Now we can compare the BEP of the MC-CDMA and DS-CDMA systems under the same conditions. Figure 4.5 shows the BEP lowerbound of these two systems. From the figure we can conclude that the MC-CDMA system can outperform the DS-CDMA system. This is mainly because that the diversity order in the frequency domain RAKE-receiver is higher than the diversity order of the time domain RAKE-receiver. In the time domain RAKE-receiver the diversity order is mainly restricted by the time resolution in the receiver and determined by the numbers of arms. In this case the number of arms is two. In the frequency domain RAKE-receivers there is no restriction on the diversity order and it is determined by the number of subcarriers.

As a consequence the DS-CDMA system with RAKE-receivers is not suitable for use in a small room, since a small room has a small rms delay. The system requires a high time resolution in the receivers.

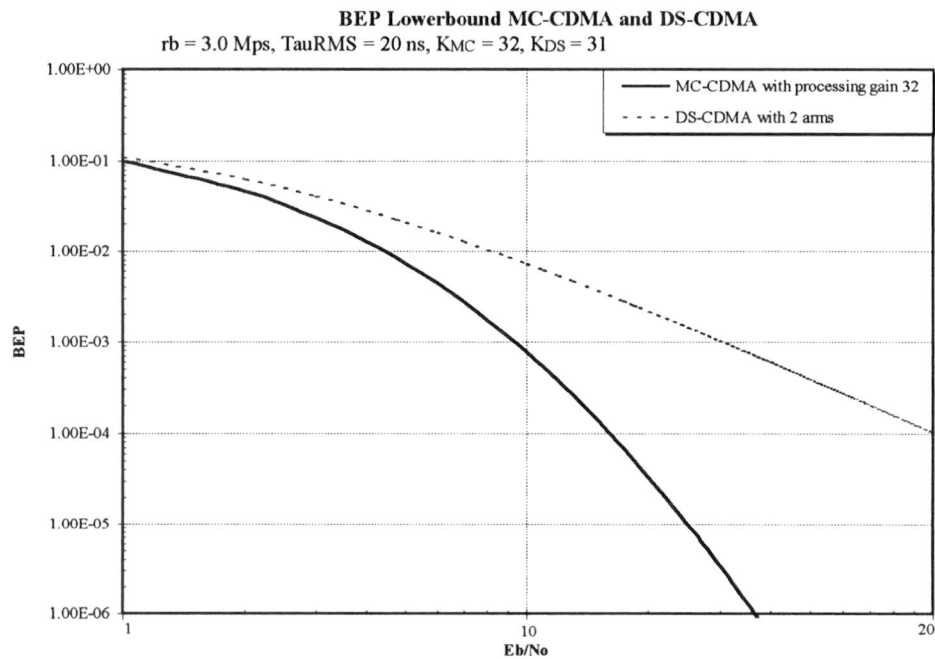


Figure 4.5 BEP comparison between MC-CDMA and DS-CDMA systems.

Computer Simulation

In this chapter computer simulation based on Monte Carlo method is carried out to verify the theoretical results for MC-CDMA system. Here we discuss the concept of Monte Carlo simulation. Besides the BEP lowerbound, the BEP upperbound and the multiuser effect on the BEP are analysed using computer simulation which have not been considered theoretically because of their complexities. The simulation program is written in C. The whole simulation program can be roughly divided into three parts: the transmitter, the channel and the receiver. In the transmitter the data are first serial-to-parallel converted before spreading over the frequency domain with the multicarrier modulator using WH codes. The channel program simulates frequency selective slow Rayleigh fading channels. We consider exponential and uniform power delay profiles. The receiver counts the number of errors in the received data sequence. In addition we propose a multiuser detection scheme to estimate the undesired information signals of the other users.

5.1 Simulation model of the transmitter

Figure 5.1 illustrates the block diagram of the base station, where the signals of the different users are multiplexed and transmitted. The data of all users are generated according to a 7-stage Maximum Sequence Length generator. We pay attention to the data transmitted by the user0. First the data are serial-to-parallel converted before spreading over the frequency

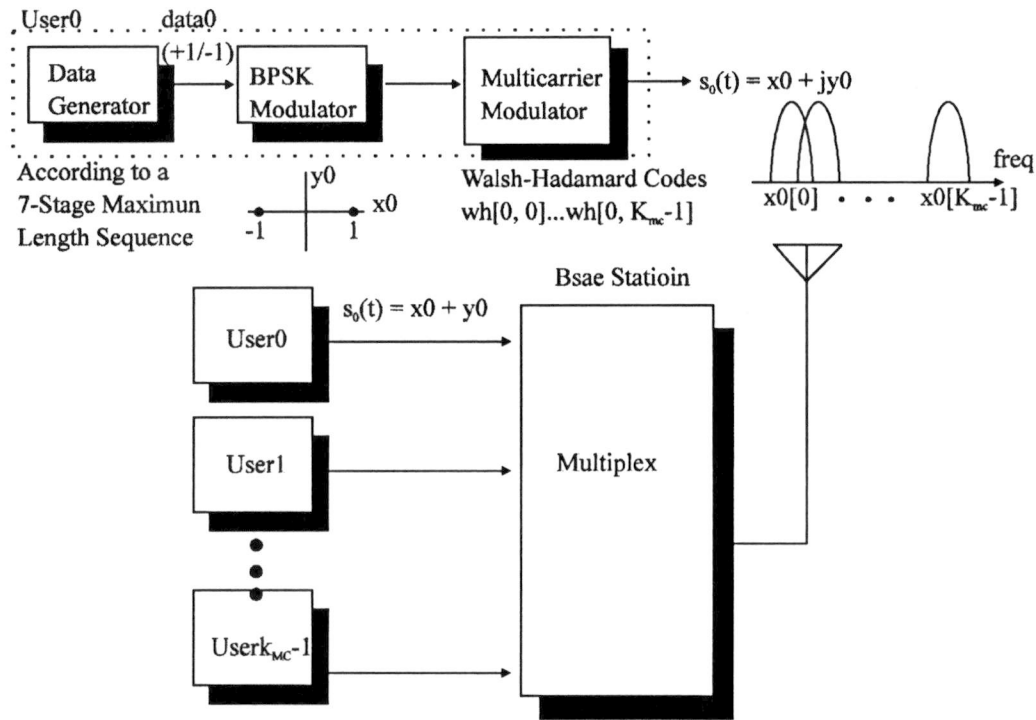


Figure 5.1 Illustration of the base station of the MC-CDMA system.

domain with the multicarrier modulator using WH codes. Then all these copies will be summed up and transmitted by user0. After the signal of user0 is received by the base station it will be multiplexed with the information signals of the other users into one signal and transmitted.

5.2 Simulation model of the channel

Through the channel the subcarriers experience frequency correlated Rayleigh fading. This is shown in figure 5.2. Also Gaussian noise is added to the signal. The channel characteristic $c(t)$ is given as $c_x + jy_2$, where c_x and c_y are two independent Gaussian random variables with zero means and variance 1/2. Then the received signal can be expressed as

$$r(t) = c(t) * s(t) + \text{complex noise} = x_2 + jy_2 \quad (5.1)$$

where $x_2 = (x_0 * c_x - y_0 * c_y) + \text{noise}$ and $y_2 = (x_0 * c_y + y_0 * c_x) + \text{noise}$. The frequency response of the channel is obtained by taking the Fourier Transform of the instantaneous channel

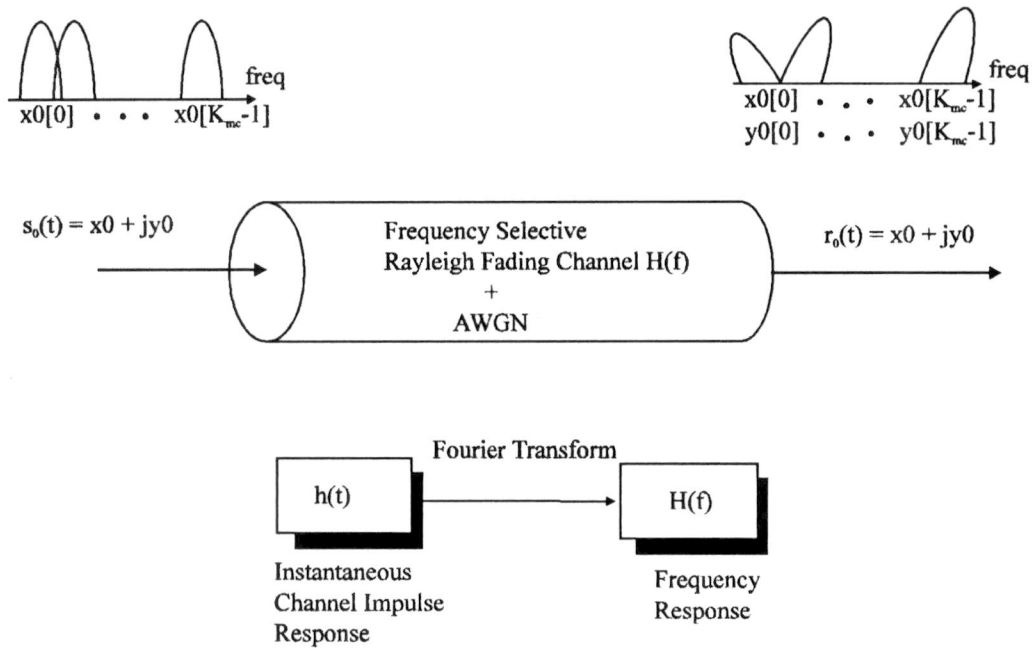


Figure 5.2 Simulation model of a frequency selective Rayleigh fading Channel.

impulse response. The orthogonality of the transmitted signal is distorted by passing through the channel.

5.3 Simulation model of the receiver

The BEP of MC-CDMA system depends on the detection scheme. Here two methods are considered: a multi-user and a single-user detection methods. Further, perfect synchronisation is assumed. The multiuser detection scheme uses the single user-detection scheme to remove the multiuser interference, therefore we first discuss the single-user detection scheme. The single-user detection scheme is based on the orthogonality restoring algorithm. Figure 5.3 shows the model of receiver0.

5.3.1 Single-User detection scheme

Using the single-user detection scheme we can achieve the worst BEP performance, which is

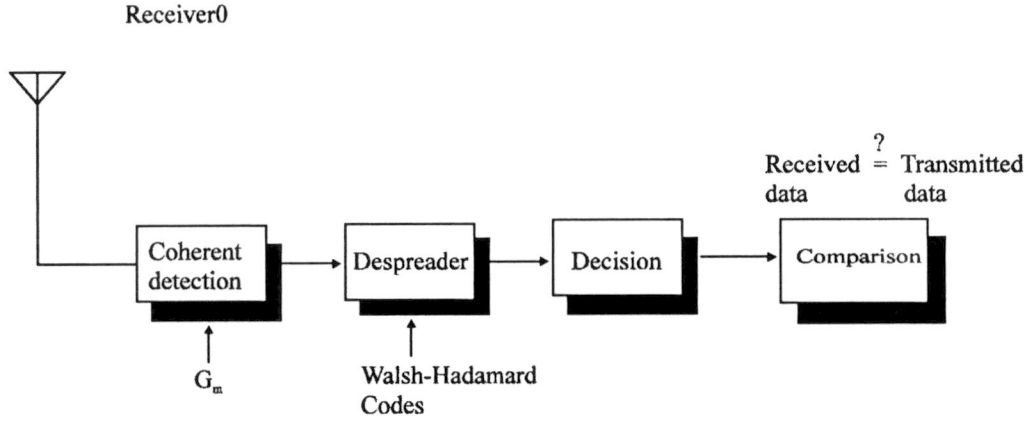


Figure 5.3 Simulation model of the MC-CDMA receiver

identical to the BEP upperbound. We choose the gain G_m as follows

$$G_m = \frac{c_m^*}{|c_m|^2} \quad (5.2)$$

Using this gain we can recover the orthogonality of the signal distorted by the channel frequency response. This process is shown in figure 5.4. Also from equation(4.19) we can see that the BEP upperbound does not depend on the number of active users.

Single-User detection algorithm

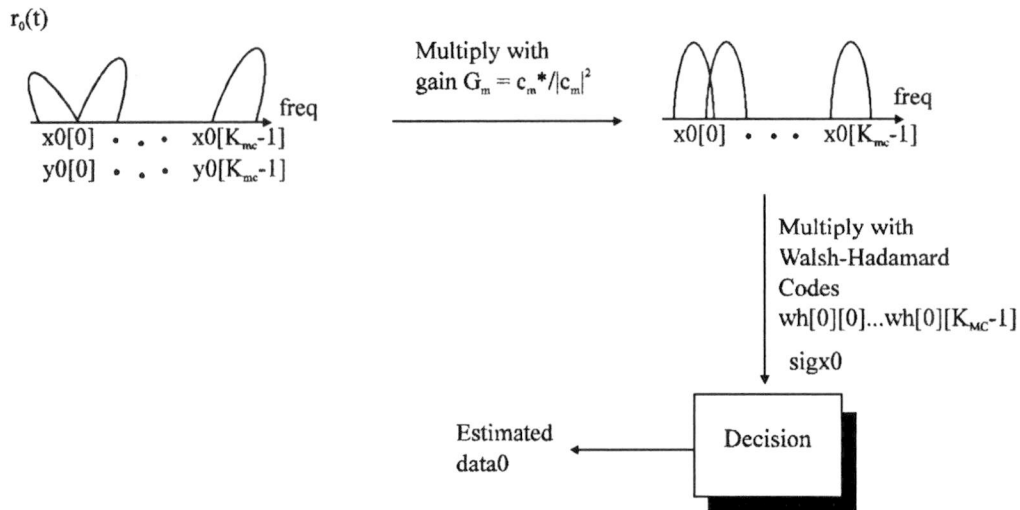


Figure 5.4 Single-user detection scheme

5.3.2 Multiuser detection method

The frequency domain RAKE-receiver combined with the simple multiuser detection scheme is shown in figure 5.4. In this scheme every user is assumed to know the code sequences of the other users. First we use the single-user detection scheme, which is based on the orthogonal restoring algorithm as discussed above, to estimate the received signals for the other users (users 1 to k). Then those signals will be subtracted from the received signal. The remaining signal will contain only the information of the desired user, in this case user0. This signal will be combined according to the frequency domain RAKE-receiver based on MRC technique. It is well known that the MRC can effectively combine the scattered signal power in the frequency domain and thus obtain the best BEP performance or the BEP lowerbound. However, since the algorithm requires that each user knows the code sequences of other active users, this detection scheme is questionable from the viewpoint of security.

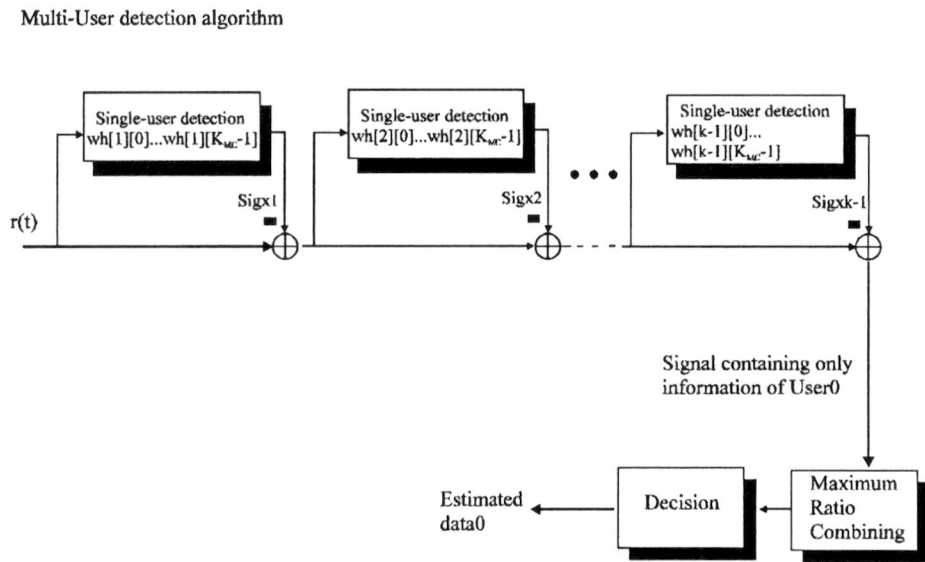


Figure 5.5 A simple multiuser detection scheme using MRC

5.4 Simulation results

Figure 5.6 shows the BEP lowerbounds and upperbounds versus E_b/N_0 for different power delay profiles: 2-path and 7-path uniform and 7-path exponential. As expected the

BEP for 7-path uniform PDP is better than that for 7-path exponential PDP because there is less correlation between the subcarriers and thus the RAKE-receiver can take the full advantages of diversity. The BEP, by assuming the 2-path uniform PDP, is clearly much worse than those using the other two PDPs.

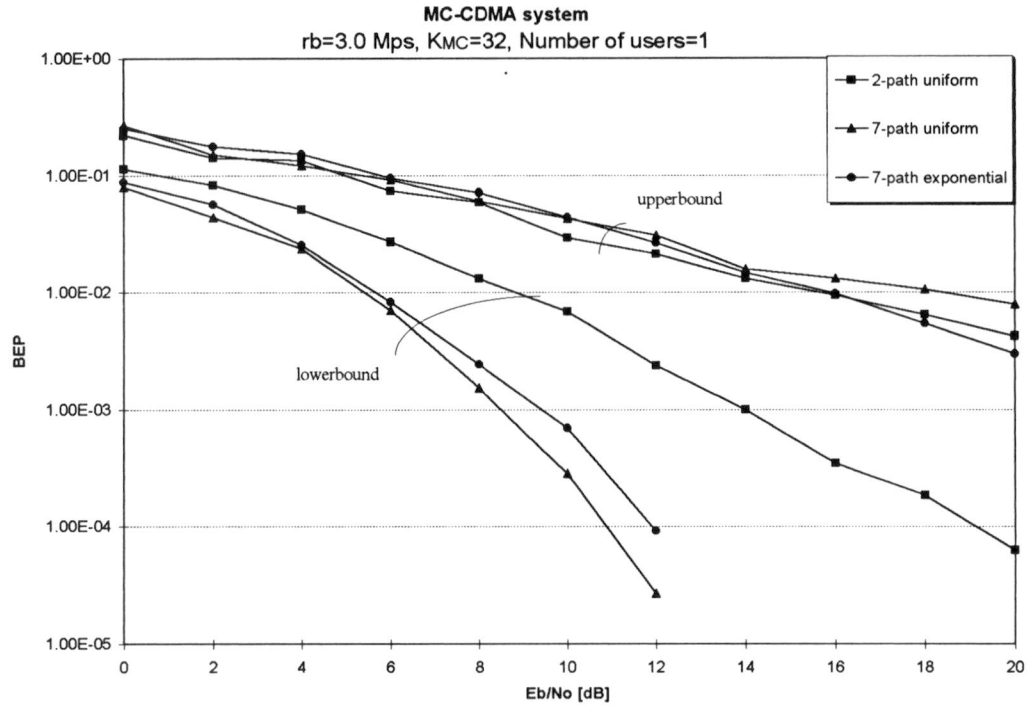


Figure 5.6 BEP lowerbounds and upperbounds for the MC-CDMA system with different PDP.

Figure 5.7 shows the effect of multi-user interference on the BEP assuming the 2-path uniform PDP. Also the BEP upperbound is shown. The BEP becomes worse as the number of simultaneous users increases.

Figure 5.8 and figure 5.9 show the BEP of the MC-CDMA system for the 7-path exponential and 7-path uniform power delay profiles respectively. The BEP performance for simultaneous two users was sometimes smaller than the BEP lowerbound. This is because of the limited simulation time used and, therefore, the accuracy is limited. Better accuracy can be obtained by taking a longer simulation time.

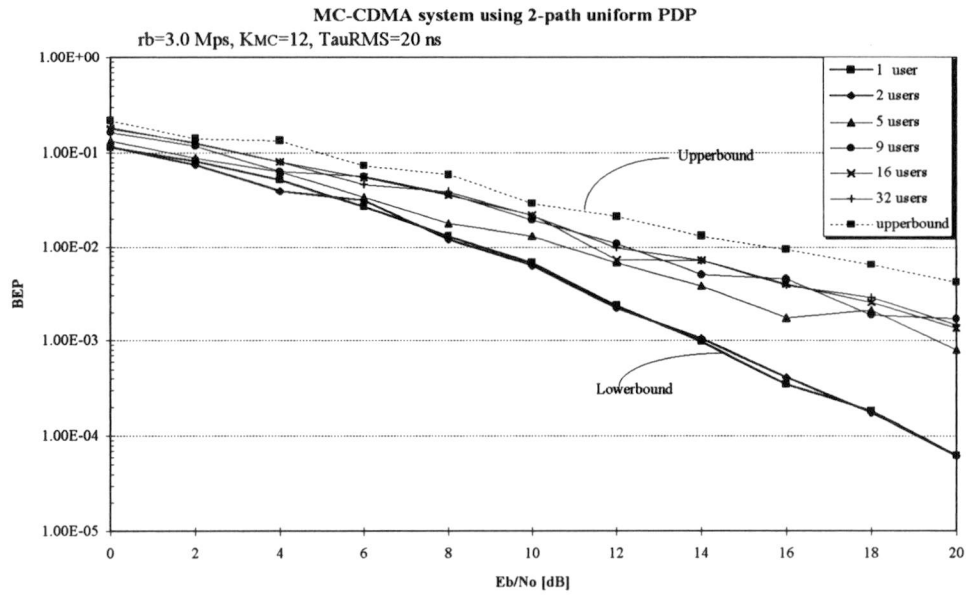


Figure 5.7 BEP for different number of users using multi-user detection scheme and MRC. 2-path uniform PDP is used.

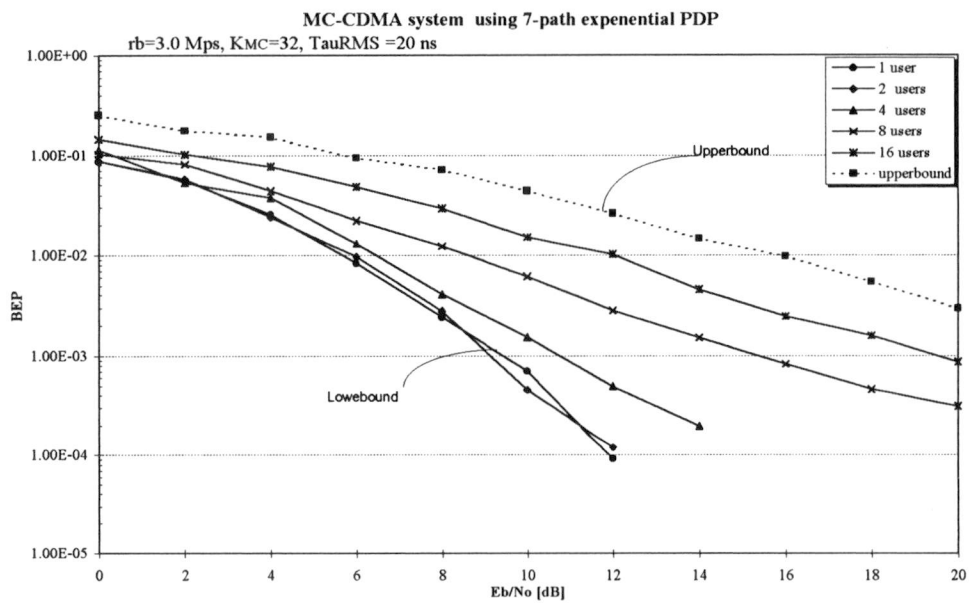


Figure 5.8 BEP for different number of users using multi-user detection scheme and MRC. 7-path exponential PDP is used.

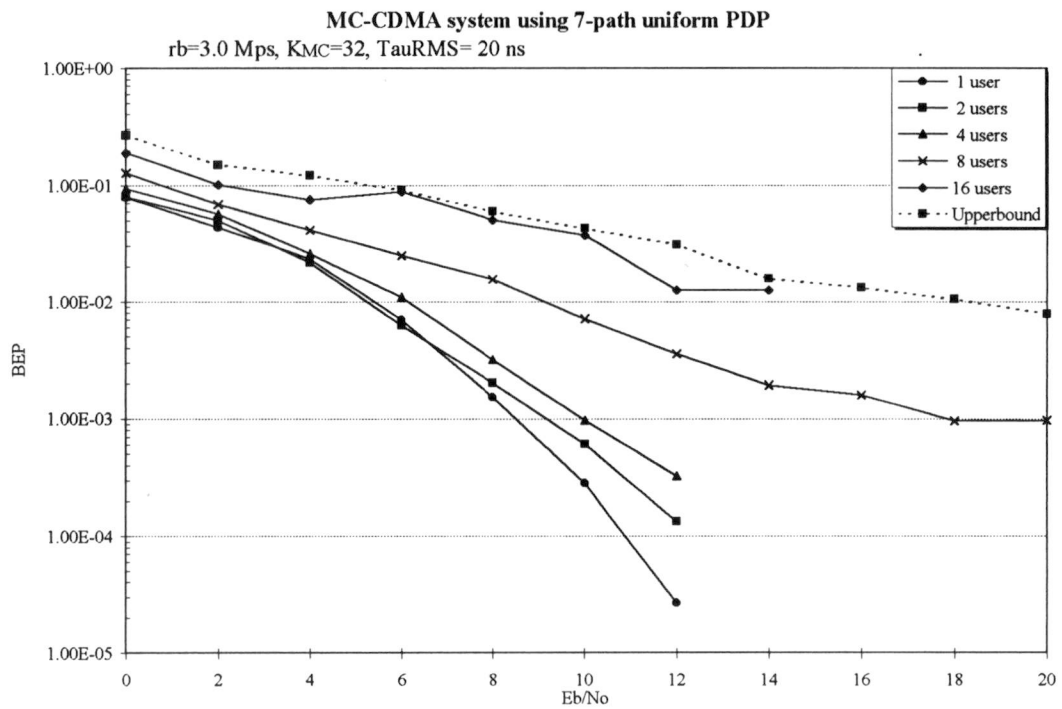


Figure 5.9 BEP for different number of users using multi-user detection scheme and MRC. 7-path uniform PDP is used.

Using the simple multi-user detection scheme fairly good performance of MC-CDMA can be obtained. Improvement in BEP performance can be expected when using more sophisticated multiuser detection schemes, such as Wiener filtering [18] and maximum-likelihood detection [19].

Figure 5.10 shows the BEP comparison between the MC-CDMA and the DS-CDMA system with different numbers of users. The BEP of the MC-CDMA system is always better than that of the DS-CDMA system. Given a bandwidth the MC-CDMA system can accommodate more users than the DS-CDMA system.

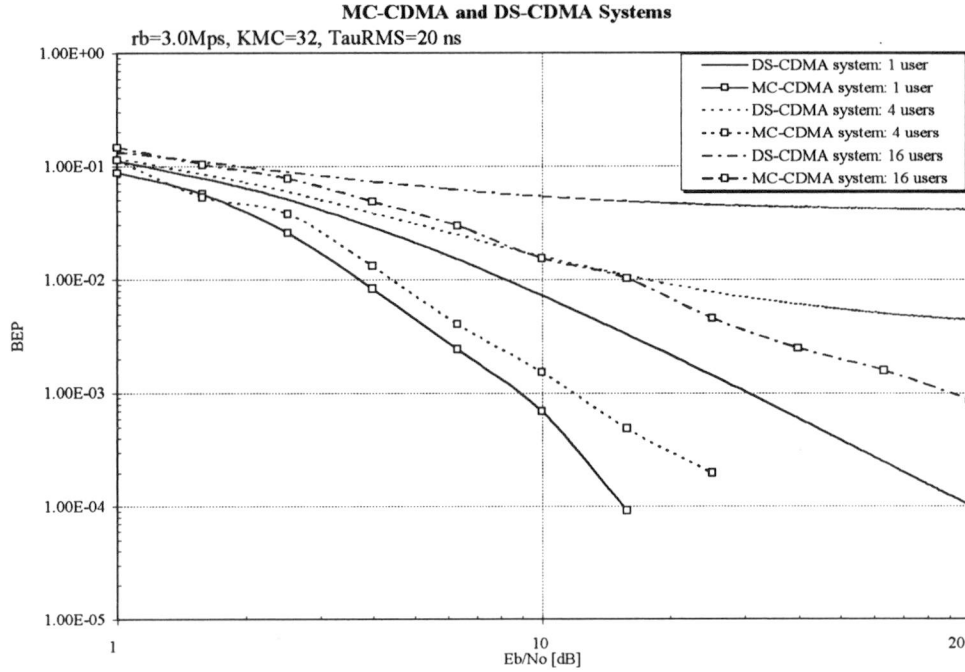


Figure 5.10 BEP comparison between MC-CDMA and DS-CDMA 7-path exponential PDP is used..

5.5 Comparison between theoretical and simulation results

Finally, we compare the results obtained by theoretical analysis and computer simulation for the exponential and uniform PDPs respectively. Figures 5.10 and 5.11 show the comparisons of BEP lowerbounds. Here we use the 7-path exponential, 2-path and 7-path uniform PDPs in the computer simulation to approximate the continuous exponential and uniform PDPs. For the case of exponential PDP, the results agree fairly well. However, for the case of uniform PDP, there are some differences between theoretical analysis and the computer simulation. The reason is that we approximate an infinite power spectrum with a discrete finite power spectrum. Clearly we need more paths in the computer simulation to obtain a better approximation for continuous uniform PDP.

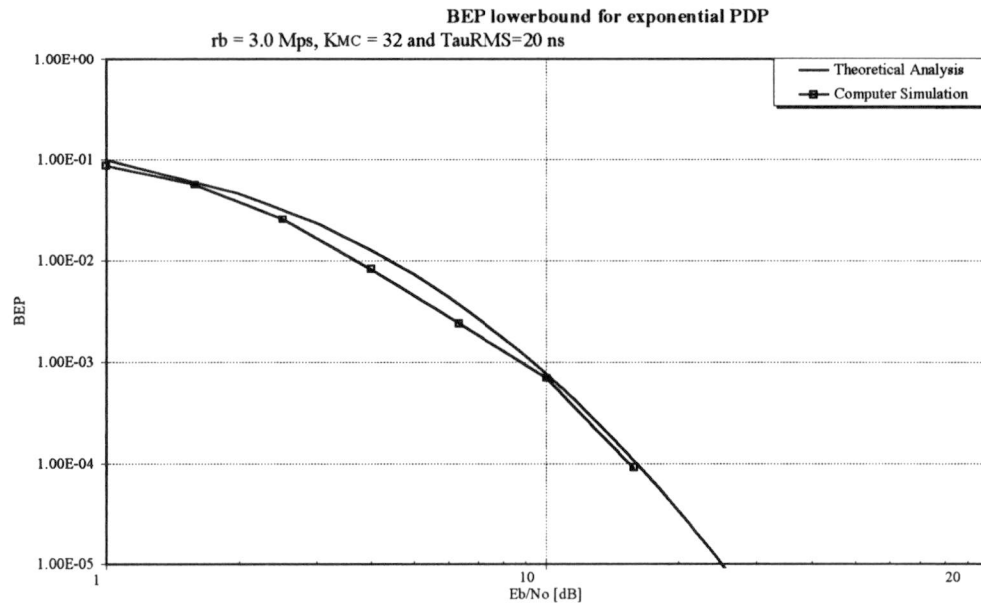


Figure 5.11 BEP lowerbound comparision between theoretical analysis and computer simulation for exponential PDP.

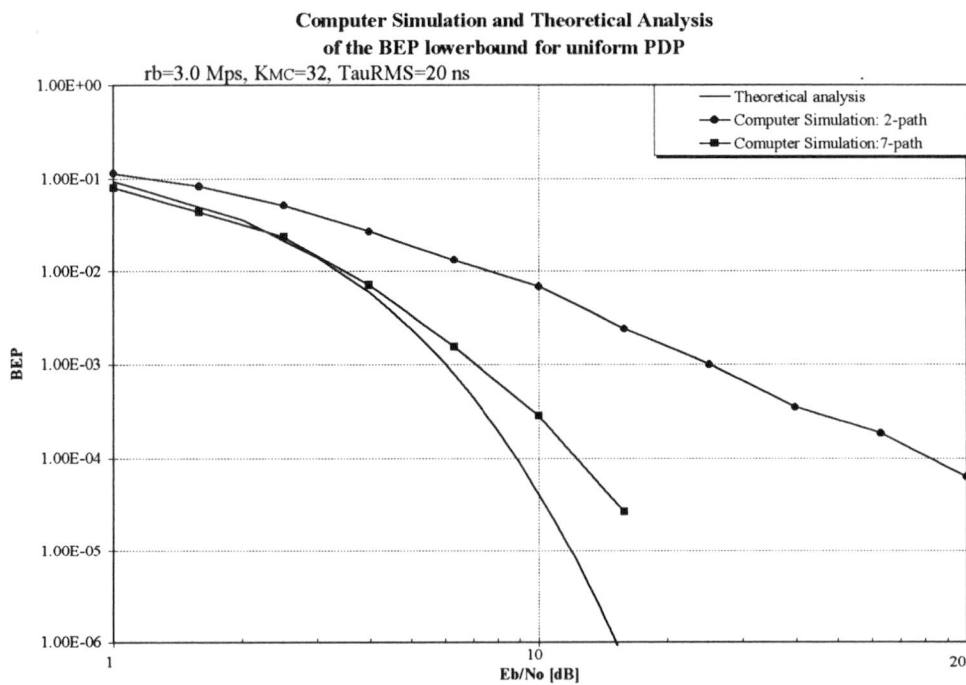


Figure 5.12 BEP lowerbound comparison between theoretical analysis and computer simulation for uniform PDP.

Conclusions and Recommendations

From the BEP lowerbounds of MC-CDMA and DS-CDMA systems, we can conclude that the MC-CDMA system can outperform the DS-CDMA system under certain circumstances, especially in a small room where the rms delay is small. This is because the diversity order in a DS-CDMA system is restricted by the time resolution in the time domain RAKE-receiver, which is determined by the chip duration T_c , while in the MC-CDMA system the diversity order is determined by the number of subcarriers.

Further, the multiuser effect on the BEP performance of the MC-CDMA has been analysed using computer simulation. A simple multiuser detection scheme is proposed. When comparing the simulation results with the theoretical results for the DS-CDMA system with simultaneous other users we can see that the MC-CDMA system can accommodate more users than the DS-CDMA system given a certain bandwidth.

For a purpose such as the implementation of the MC-CDMA system frequency selective fading channel model should be used instead of frequency non-selective fading channel model. Because frequency non-selective fading channels model will give too optimistic results compared to frequency selective fading channel model.

The BEP lowerbounds for the MC-CDMA system obtained by theoretical and computer simulation agree well.

Also the BEP upperbound of the MC-CDMA system has been analysed using computer simulation. This upperbound is independent of the number of users.

The BEP becomes better when the rms delay spread increases for both CDMA system. This is because the received signals are more uncorrelated so we can take a better advantage of diversity when using RAKE-receivers.

Recommendations:

- In this report a simple multiuser detection scheme has been proposed. We can use another multiuser detection scheme to improve the BEP performance, such as the Wiener filtering detection and the maximum-likelihood detection.
- Synchronisation of the FFT windows has not been taken into account and it is important to consider it in practical systems.
- A longer simulation time can be taken in order to improve the accuracy.
- A Rician fading channel can be considered, for example by using computer simulation.
- Error correcting codes can be considered in the MC-CDMA system in order to improve the system performance.

References

- [1] G.J.M. Janssen and R. Prasad
Propagation measurement in an indoor radio environment at 2. GHz, 4.75GHz and 11.5Ghz
Vehicular Technology Society 42nd VTS conference frontiers of Technology, May 10-13, 1992, Denver, Colorado, pp. 617-620
- [2] A.M. saleh and R.A. Valenzuela
A statistical indoor model for indoor multipath propagation
IEEE Journal on Selected Areas in Communications, SAC-5, pp. 128-137, Feb. 1992
- [3] N. Yee, J.P. Linnartz and G. Fettweis
Multi-carrier CDMA in Indoor Wireless Radio Networks
Proceedings PIMRC '93, Yokohama, Japan, 1993, pp. 109-113
- [4] J.G. Proakis
Digital Communication
McGraw-Hill International Editions, Computer Science Serires, Second edition 1989
- [5] M. Schwartz, W.R. Benntt and S. Stein
Communication Systems and Techniquese
McGraw-Hill Book Company, 1966
- [6] W.C.Jakes
Microwave Mobile Communnications
Wiley, New York, 1974
- [7] M.J. Gans
A Power Spectral Theory of Propagation in the Mobile Radio Environment.
IEEE Transaction on Vehicular Technology, Vol. 21, Feb 1972

- [8] A.B. Carlson
Communication Systems
McGraw-Hill Book Company, third edition, 1988

- [9] I. Widipangestu, A. J. 'T Jong, and R. Prasad
Capture Probability and Throughput Analysis of Slotted ALOHA and Unslotted np-ISMA in a Rician/ Rayleigh Environment
IEEE Transaction on Vehicular Technology, Vol. 43, No. 3, Aug. 1994

- [10] F.D. Garber and M.B. Pursley
Performance of the Differentially Coherent Digital Communications Over Frequency-Selective Fading Channel
IEEE Transaction on Communcations, Vol. 36, No. 1, Jan. 1988

- [11] A.A.M. Saleh and R.A. Valenzuela
A Statistical Model for Indoor Multipath Propagation
IEEE Journal on Selected Areas in Commuications, Vol. SAC-5, No. 2, Feb 1987

- [12] M.B. Pursley
Performance Evaluation for Phase-Coded Spread-spectrum Multiple -Access Communication-Part I: System Analysis.
IEEE Transactions on Communcations, Vol. COM-25, No. 8. Aug. 1977

- [13] R.L. Pickholtz, D.L. Schilling and L.B. Milsten
Theory of Spread-Spectrum Communications- A Tutorial
IEEE Transactions on Communications, Vol. COM-30, No. 5, May 1982

- [14] W.Y.C. Lee
Overview of Cellular CDMA
IEEE Transactions on Vehicular Technology, Vol. 40, No. 2, May 1991

- [15] J.C. Arnbak and W. Blitterswijk
Capacity of Slotted ALOHA in Rayleigh-Fading Channels
IEEE Journal on Selected Areas in Communnication, Vol. SAC-5, No. 2 February 1987

- [16] R. Prasad and C.Y. Liu
Throughput analysis of some mobile packet radio protocols in Rician fading channels
IEEE Proceedings-I, Vol. 139, No. 3, June 1992

- [17] S. Hara, M. Mouri, M. Okada and N. Morinaga
Transmission Performance Analysis of Multi-carrier Modulation in Frequency Selective Fast Rayleigh fading Channel
accepted for publication in Wireless Personal Communications: An International Journal, Special Issue on Multi-Carrier communications, Kluwer Academic Publishers

- [18] N.Yee and J-P.Linnartz
Wiener Filtering of Multi-Carrier CDMA in a Rayleigh Fading Channel
Proceedings of IEEE PIMRC'94, pp.1344-1347, The Hague, The Netherlands, Sept. 1994.

- [19] Y.Bar-Ness, J-P.Linnartz and X.Lin
Synchronous Multi-User Multi-Carrier CDMA Communication System with Decorrelating Interference Canceler
Proceedings of IEEE PIMRC'94, pp.184-188, The Hague, The Netherlands, Sept. 1994.

Appendix:

BER Comparison of DS-CDMA and MC-CDMA for Frequency Selective Fading Channels

7th Tyrrhenian International Workshop on digital Communications 10-14 September 1995

BER Comparison of DS-CDMA and MC-CDMA for Frequency Selective Fading Channels

Shinsuke Hara[†], Tai-Hin Lee[‡] and Ramjee Prasad[‡]

[†]Department of Communication Engineering, Faculty of Engineering,
Osaka University,

2-1, Yamada-oka, Suita-shi, Osaka 565 Japan,

E-MAIL : hara@comm.eng.osaka-u.ac.jp

[‡]Telecommunications and Traffic-Control Systems Group,

Delft University of Technology,

P.O.Box 5031, 2600GA, Delft, The Netherlands

Abstract: This paper presents the advantages and disadvantages of DS-CDMA (Direct Sequence-Code Division Multiple Access) and MC-CDMA (Multi-Carrier-Code Division Multiple Access) systems in synchronous down-link mobile radio communication channels. Furthermore, the bit error rate (BER) performance is analyzed in frequency selective slow Rayleigh fading channels. We theoretically derive the BER lower bound for MC-CDMA system, and propose a simple multi-user detection method. In the BER analysis, we use the same multipath delay profiles for both DS-CDMA and MC-CDMA systems, and discuss the performance theoretically and by computer simulation. Finally, we theoretically prove that the time domain DS-CDMA Rake receiver is equivalent to the frequency domain MC-CDMA Rake receiver for the case of one user.

1 Introduction

Direct Sequence-Code Division Multiple Access (DS-CDMA) technique has been considered to be a candidate to support multi-media services in mobile communications, because it has its own capabilities to cope with asynchronous nature of multi-media data traffic, to provide higher capacity over conventional access techniques such as TDMA and FDMA, and to combat the hostile channel frequency selectivity.

Recently, another CDMA technique based on a combination of the CDMA and the orthogonal frequency division multiplexing (OFDM) signaling has been reported in [1],[2]. This technique is called "Multi-Carrier-CDMA (MC-CDMA) technique", and much attention has been paid to it, because it is potentially robust to the channel frequency selectivity with a good frequency utilization efficiency.

In the bit error rate (BER) analysis of DS-CDMA system, "independent fading characteristic at each received path" is assumed, on the other hand, "independent fading characteristic at each sub-carriers" is considered in the BER analysis of MC-CDMA system[1],[2]. When the multipath channel is a wide sense stationary uncorrelated scattering (WSSUS) one, the assumption for the DS-CDMA system is correct, however, the

assumption for the MC-CDMA system is not correct. In the BER analysis of MC-CDMA system, we should take account of frequency correlation function determined by the multipath delay profile of the channel, and in the BER comparison, we should make a fair assumption for both DS-CDMA and MC-CDMA systems using the same channel frequency selectivity, that is, the same multipath delay profile. To the best of the authors' knowledge, no paper has been reported on the fair BER comparison.

In this paper, we discuss the advantages and disadvantages of DS-CDMA and MC-CDMA systems in synchronous down-link mobile radio communication channels, and analyze the bit error rate (BER) performance in frequency selective slow Rayleigh fading channels theoretically and by computer simulation. Section 2 explains the DS-CDMA and MC-CDMA systems and discusses the advantages and disadvantages of MC-CDMA system over DS-CDMA system. Section 3 shows the theoretical derivation of BER lower bound for the MC-CDMA system, and proposes a simple multi-user detection method. Section 4 discusses the BER performance in frequency selective slow Rayleigh fading channels. Section 5 theoretically proves the equivalence of time domain DS-CDMA Rake receiver and frequency domain MC-CDMA Rake receiver for the case of one user. Section 6 draws the conclusions.

2 DS-CDMA and MC-CDMA Systems

2.1 DS-CDMA System

DS-CDMA transmitter spreads the original signal using a given spreading code in the time domain (see Fig.1). The capability of suppressing multi-user interference is determined by the cross-correlation characteristic of the spreading codes. Also, a frequency selective fading channel is characterized by the superimposition of several signals with different delays in the time domain[3]. Therefore, the capability of distinguishing one component from

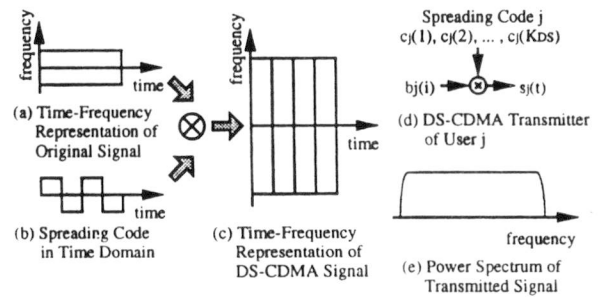


Fig. 1: Concept of DS-CDMA System

other components in the composite received signal (time resolution) is determined by the auto-correlation characteristic of the spreading codes.

Fig.1(d) shows the DS-CDMA transmitter of the j -th user for Binary PSK modulation/coherent demodulation (CBPSK) scheme. The complex equivalent low-pass transmitted signal is written by

$$s_j(t) = \sum_{i=-\infty}^{+\infty} \sum_{k=1}^{K_{DS}} b_j(i) c_j(k) p(t - kT_c - iT_s), \quad (1)$$

where, $b_j(i)$ and $c_j(k)$ are the i -th information and the k -th bit of the spreading code with length K_{DS} and chip duration T_c , respectively, T_s is the symbol duration, and $p(t)$ is the pulse waveform defined as:

$$p(t) = \begin{cases} 1 & (0 \leq t \leq T_c) \\ 0 & (\text{otherwise}). \end{cases} \quad (2)$$

The BER is determined by the path diversity strategy in the receiver, and the diversity order depends on how many fingers the Rake receiver employs. Usually, the diversity order of 1 (Non-Rake), 2 or 3 is used depending on hardware limitation. Furthermore, when the Nyquist filters are introduced in the transmitter and receiver for base band pulse shaping, the Rake receiver may wrongly combine paths. This is because noise causing distortion in auto-correlation characteristic often results in wrong correlation. Finally, it is difficult for the DS-CDMA Rake receiver to use all the received signal energy scattered in the time domain.

2.2 MC-CDMA System

The MC-CDMA transmitter spreads the original signal using a given spreading code in the frequency domain (see Fig.2). It is crucial for multi-carrier transmission to have frequency non-selective fading over each sub-carrier. Therefore, if the original symbol rate is high enough to become subject to frequency selective fading, the signal needs to be first serial-to-parallel converted before spreading over the frequency domain. Also, in a synchronous down-link mobile radio communication channel, we can use the Hadamard Walsh codes as an optimum orthogonal code set, because we do not have to pay attention to the auto-correlation characteristic of the spreading codes.

Fig.3(a) shows the MC-CDMA transmitter of the j -th user for CBPSK scheme, where the input information sequence is converted into P parallel data sequences ($a_{j,1}(i)$, $a_{j,2}(i), \dots, a_{j,P}(i)$). The complex equivalent low-pass transmitted signal is written by

$$s_j(t) = \sum_{i=-\infty}^{+\infty} \sum_{p=1}^P \sum_{m=1}^{K_{MC}} a_{j,p}(i) d_{m,p}^j p(t - iT_s) e^{j2\pi\Delta f(m + \frac{p-1}{P})t}, \quad \Delta f = 1/T_s, \quad (3)$$

where $\{d_1^j, d_2^j, \dots, d_{K_{MC}}^j\}$ is the Hadamard Walsh code for the j -th user (the length is K_{MC}) and Δf is the sub-carrier separation for $a_{j,p}(i)$. Also, the total number of sub-carriers is $P \times K_{MC}$.

2.3 Advantages and Disadvantages

2.3.1 Advantages of MC-CDMA System over DS-CDMA System

We define the following parameters:

- Transmission Rate : $R (= 1/T_s)$ [bits/sec],
- Processing Gain : K_{DS} (DS-CDMA), K_{MC} (MC-CDMA),
- The Maximum Number of Users : M_{DS} (DS-CDMA), M_{MC} (MC-CDMA),

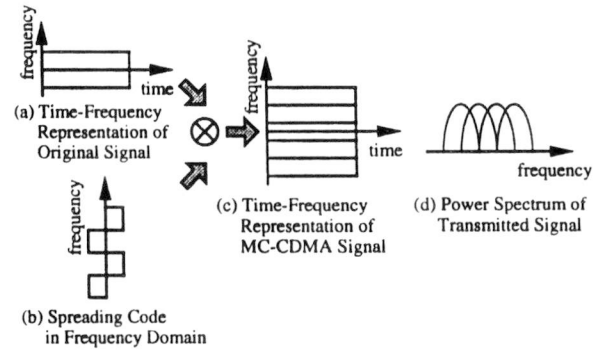


Fig. 2: Concept of MC-CDMA System

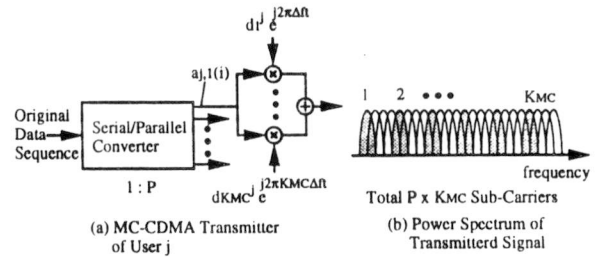


Fig. 3: MC-CDMA Transmitter of User j

- The Number of Sub-Carriers : $N (= P \times K_{MC})$.

The required frequency bandwidth (main-lobe) for the DS-CDMA system becomes

$$B_{DS} = 2 \cdot R \cdot K_{DS}, \quad (4)$$

on the other hands, for the MC-CDMA system,

$$B_{MC} = R \cdot K_{MC} \cdot (N + 1)/N \approx R \cdot K_{MC}. \quad (5)$$

From Eqs.(4) and (5),

$$K_{MC} = 2 \cdot K_{DS} \quad \text{if} \quad B_{MC} = B_{DS}. \quad (6)$$

Eq.(6) shows that the processing gain of MC-CDMA system is twice as large as that of DS-CDMA system for a given frequency bandwidth. Furthermore, the DS-CDMA system cannot accommodate K_{DS} users ($M_{DS} < K_{DS}$) because we need to choose the spreading codes with good auto- and cross-correlation characteristics carefully, while the MC-CDMA system can accommodate K_{MC} users ($M_{MC} = K_{MC}$) using the Walsh Hadamard codes:

$$M_{MC} > 2 \cdot M_{DS} \quad \text{if} \quad B_{MC} = B_{DS}. \quad (7)$$

2.3.2 Disadvantages of MC-CDMA System over DS-CDMA System

At the MC-CDMA receiver, we have to make every effort in the FFT window position synchronization, the frequency offset compensation and the coherent detection at each sub-carrier. Also, the MC-CDMA transmitter requires a large input backoff in the amplifier, because it is very sensitive to nonlinear amplification.

It is also pointed out that the BER of multi-carrier modulation itself is inferior to that of single-carrier modulation mainly due to the power loss associated with guard interval insertion[4].

3 BER Analysis

3.1 Frequency Selective Slow Rayleigh Fading Channel Model

We assume a wide sense stationary uncorrelated scattering (WSSUS) channel model[3] with L received paths in the complex equivalent low-pass time-variant impulse response:

$$h(\tau; t) = \sum_{l=1}^L g_l(t) \delta(\tau - \tau_l). \quad (8)$$

where t and τ are the time and the delay, respectively, $\delta(t)$ is the Dirac delta function, $g_l(t)$ is the complex envelope of the signal received on the l -th path which is a complex Gaussian random process with zero mean and variance σ_l^2 , and τ_l is the propagation delay for the l -th path.

Fig.4 shows the corresponding multipath delay profile given by

$$\phi_c(\tau) = \frac{1}{2} E [h^*(\tau; t) \cdot h(\tau; t)] = \sum_{l=1}^L \sigma_l^2 \delta(\tau - \tau_l), \quad (9)$$

where $E[\cdot]$ is the expectation.

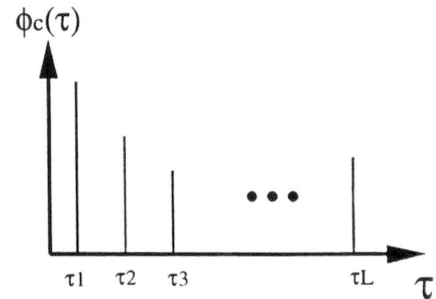


Fig. 4: Multipath Delay Profile

3.2 Communication System Model

We consider a synchronous down-link communication channel, where the signal is transmitted in a burst format with a preamble and a postamble. In this paper, we assume that the receiver can correctly estimate all the channel state information.

3.3 BER of DS-CDMA System

The transmitted signal for total J users is written by

$$s(t) = \sum_{j=1}^J s_j(t). \quad (10)$$

The received signal through the frequency selective slow Rayleigh fading channel given by Eq.(8) is written by

$$r(t) = \int_{-\infty}^{+\infty} s(t - \tau) * h(\tau; t) d\tau + n(t) = \sum_{l=1}^L r_l(t) + n(t), \quad r_l(t) = s(t - \tau_l) g_l(t), \quad (11)$$

where $n(t)$ is the complex additive Gaussian noise. Defining \mathbf{r}_t as the received signal vector, the time domain covariance matrix \mathbf{M}_t is given by

$$\mathbf{r}_t = [r_1, r_2, \dots, r_L]^T, \quad \mathbf{M}_t = \frac{1}{2} E [\mathbf{r}_t \cdot \mathbf{r}_t^T] = \begin{bmatrix} \sigma_1^2 & 0 & \dots & 0 \\ 0 & \sigma_2^2 & & \vdots \\ \vdots & & \ddots & 0 \\ 0 & \dots & 0 & \sigma_L^2 \end{bmatrix}, \quad (12)$$

where T is the transpose. In the above equation, we assume a perfect auto-correlation characteristic for the spreading codes.

The BER of time domain I -finger DS-CDMA Rake receiver is uniquely determined by the eigenvalues of \mathbf{M}_t (in this case, the eigenvalues are clearly $\sigma_1^2, \sigma_2^2, \dots, \sigma_L^2$) [5]. For example, when σ_l^2 ($l = 1, \dots, L$) are different each other, the BER is expressed as

$$BER = \sum_{l=1}^I w_l \cdot \frac{1}{2} \left\{ 1 - \sqrt{\frac{\sigma_l^2/N'}{1 + \sigma_l^2/N'}} \right\}, \quad w_l = \frac{1}{\prod_{\substack{n=1 \\ n \neq l}}^I \left(1 - \frac{\sigma_n^2}{\sigma_l^2} \right)}, \quad (13)$$

$$E_b = \sum_{l=1}^L \sigma_l^2, \quad N' = N_0 + \frac{2(J-1)}{3K_{DS}} E_b, \quad (14)$$

where E_b and N_0 are the signal energy per bit and the noise spectral density, respectively. Also, when σ_l^2 ($l = 1, \dots, L$) are all the same ($= \sigma^2$) [3],

$$BER = \left(\frac{1 - \mu}{2} \right)^I \sum_{l=0}^{I-1} \binom{I-1+l}{l} \left(\frac{1 + \mu}{2} \right)^l, \quad \mu = \sqrt{\frac{\sigma^2/N'}{1 + \sigma^2/N'}}. \quad (15)$$

Eqs.(13) and (15) are based on the Gaussian approximation for multi-user interference[6].

3.4 BER of MC-CDMA System

The transmitted signal for total J users is written by

$$s(t) = \sum_{j=1}^J s_j(t). \quad (16)$$

The received signal through the frequency selective slow Rayleigh fading channel is written by

$$r(t) = \sum_{i=-\infty}^{+\infty} \sum_{p=1}^P \sum_{m=1}^{K_{MC}} \sum_{j=1}^J z_{m,p} a_{j,p}(i) d_m^j p(t - iT_s) e^{j2\pi\Delta f(m+\frac{p-1}{P})t} + n(t), \quad (17)$$

where $z_{m,p}$ is the complex received signal at the $(mP + p - 1)$ -th sub-carrier.

Fig.5 shows the MC-CDMA receiver of the j' -th user, where after the serial-to-parallel conversion using the FFT, the m -th sub-carrier component for the received data $a_{j,p}(i)$ is multiplied by the gain G_m and despreading code $d_m^{j'}$ to combine the energy of received signal scattered in the frequency domain. The decision variable is given by (we can omit the subscriptions p and i without loss of generality)

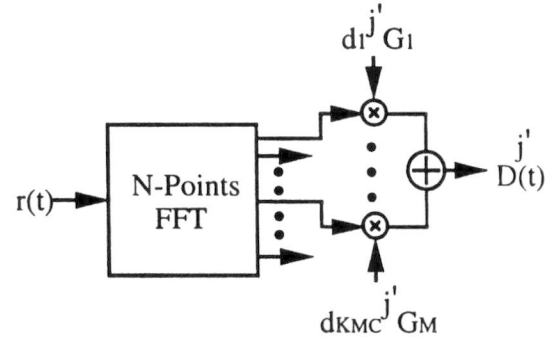


Fig. 5: MC-CDMA Receiver of the j' -th user

$$D^{j'}(t) = \sum_{m=1}^{K_{MC}} \sum_{j=1}^J G_m d_m^{j'} \{z_m a_j d_m^j + n_m(t)\}, \quad (18)$$

where $n_m(t)$ is the complex additive Gaussian noise at the m -th sub-carrier.

3.4.1 Orthogonality Restoring Single-User Detection Method

Choosing the gain G_m as

$$G_m = z_m^* / |z_m|^2, \quad (19)$$

the receiver can eliminate the multi-user interference perfectly. However, low-level sub-carriers tend to be multiplied by the high-gains, so the BER degrades due to noise amplification (a weak signal suppression method using a detection threshold is presented in [8]).

3.4.2 Frequency Domain Rake Receiver with No Simultaneous Other User

When there is no simultaneous other user, the frequency domain MC-CDMA Rake receiver based on the maximum ratio combining method in the frequency domain ($G_m = z_m^*$) can achieve the best BER performance (the BER lower bound)[3].

Defining \mathbf{r}_f as the received signal vector, the frequency domain covariance matrix \mathbf{M}_f is given by

$$\mathbf{r}_f = [z_1, z_2, \dots, z_{K_{MC}}]^T, \quad \mathbf{M}_f = \frac{1}{2} E [\mathbf{r}_f \cdot \mathbf{r}_f^T] = \{m_f^{a,b}\}, \quad (20)$$

$$m_f^{a,b} = \Phi_C((a-b)\Delta f), \quad (21)$$

where $m_f^{a,b}$ is the $a - b$ element of \mathbf{M}_f , and $\Phi_C(\Delta f)$ is the spaced frequency correlation function defined as the Fourier transform of the multipath delay profile given by Eq.(9):

$$\Phi_C(\Delta f) = \int_{-\infty}^{+\infty} \phi_c(\tau) e^{-j2\pi\Delta f\tau} d\tau. \quad (22)$$

Defining $\lambda_1, \lambda_2, \dots, \lambda_{K_{MC}}$ as the eigenvalues of \mathbf{M}_f , the BER is given by a form similar to Eq.(13) or Eq.(15)[5], where we can substitute I , N' , L and σ^2 for K_{MC} , N_0 , K_{MC} and λ , respectively.

3.4.3 Simple Multi-User Detection Method

In this paper, we propose a simple multi-user detection method. If the preamble contains information on the spreading codes used by the simultaneous users, any user can know it easily (although providing multi-user information in the down-link channel is questionable from the viewpoint of security). In this method, the user first estimates information for simultaneous other $J - 1$ users using the orthogonality restoring single-user detection method. After removing the interference component from the received signal, the user detects its own information using the frequency domain maximum ratio combining method. If the decisions for the other users are correct, this detection method can minimize the BER.

4 Numerical Results

We assume the following system parameters to demonstrate the BER performance: $\bullet R = 3.0[\text{Mbits/sec}]$, $\bullet K_{DS} = 31(\text{Gold Codes})$, $\bullet K_{MC} = 32$.

4.1 BER Performance of DS-CDMA System

Figs.6, 7 and 8 show the BER performance of DS-CDMA system in frequency selective slow Rayleigh fading channels with 2-path uniform, 7-path uniform and 7-path exponential multipath delay profiles, respectively. All the delay profiles have the same RMS delay spread $\tau_{RMS}=20[\text{nsec}]$.

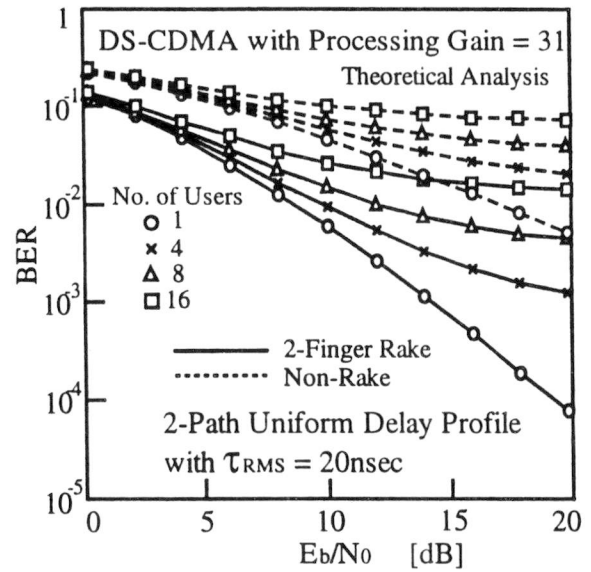


Fig. 6: BER of DS-CDMA System (2-Path Uniform Delay Profile)

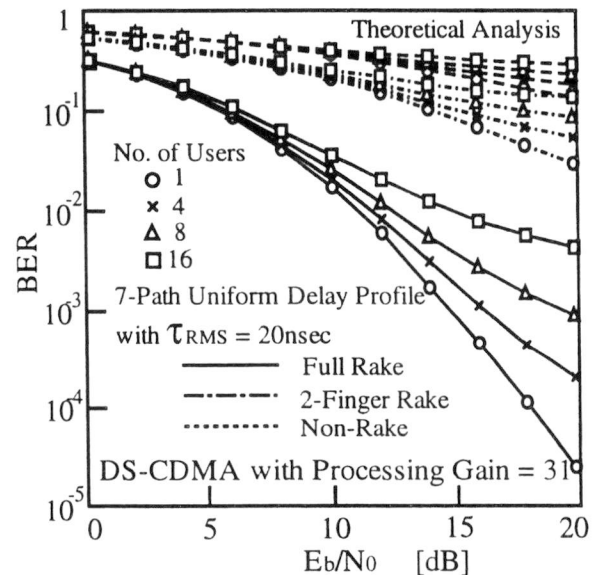


Fig. 7: BER of DS-CDMA System (7-Path Uniform Delay Profile)

As compared with the full-finger Rake receiver, the performance of Non-Rake receiver is poor. For the delay profiles where several delayed paths have the same average power as the first path, there is a large difference in the attainable BER between the Non-Rake and full-finger Rake receivers. Also, as the number of users increases, the performance gradually degrades. For the 7-path uniform and exponential multipath delay profiles, the full-finger Rake receiver means 7-finger Rake receiver. From the practical point of view, its realization could be difficult.

4.2 Design of MC-CDMA System

As the number of sub-carriers (N) increases, the transmission performance becomes more sensitive to the time selectivity because the wider symbol duration is less robust to the random FM noise. On the other hand, as N decreases, it becomes poor because the wider power spectrum of each sub-carrier is less robust to the frequency selectivity. Therefore, there exists an optimum value in N to minimize the BER[9].

Also, as the guard duration (Δ) increases, the transmission performance becomes poor because the signal transmission in the guard duration introduces the power loss. On the other hand, as Δ decreases, it becomes more sensitive to the frequency-selectivity because the shorter guard duration is less robust to the delay spread. Therefore, there exists an optimum value in Δ to minimize the BER[9].

In [9], it is shown that when the product of the maximum Doppler frequency f_D and the root mean square delay spread τ_{RMS} introduced in the channel satisfies the following condition:

$$\tau_{RMS} \cdot f_D < 1.0 \times 10^{-6}, \quad (23)$$

the multi-carrier modulation scheme can achieve almost the same BER performance as a single-carrier modulation scheme with equalization.

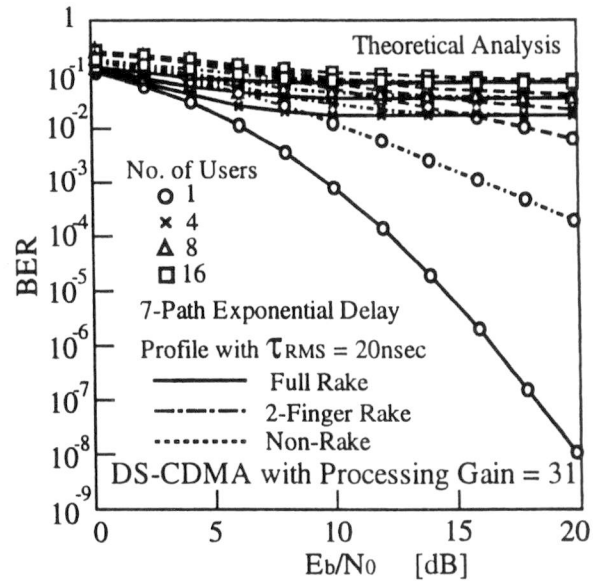


Fig. 8: BER of DS-CDMA System (7-Path Exponential Delay Profile)

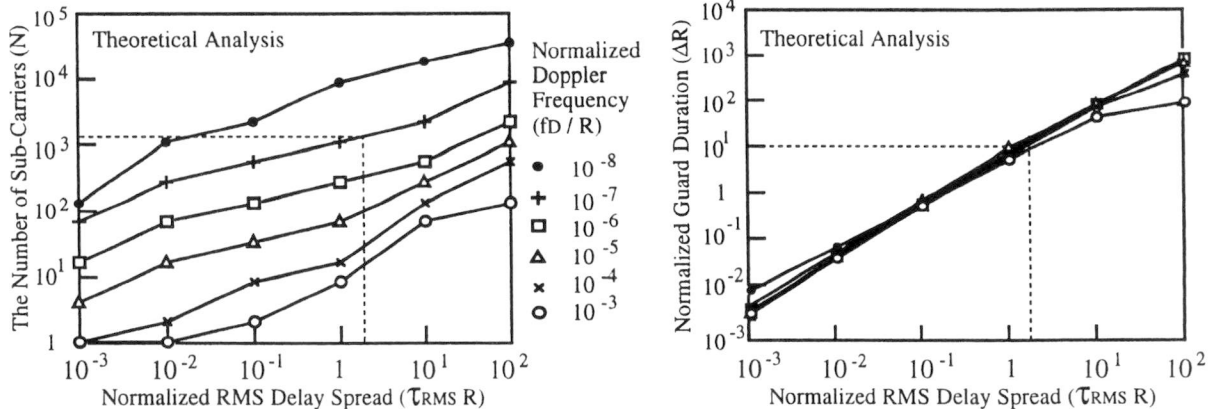


Fig. 9: Design of The Number of Sub-Carriers and Guard Period

Fig.9 shows the optimum values of the number of sub-carriers and guard period for $f_D = 10[\text{Hz}]$ and $\tau_{RMS} = 20[\text{nsec}]$. The MC-CDMA system with $N = 1024$ and $\Delta = 100[\text{nsec}]$ can minimize the BER, where the original information sequence is first converted into 32 parallel sequences ($P=32$), and then each sequence is mapped onto 32 sub-carriers. Also, the power loss associated with guard period insertion is negligible small (the normalized guard duration is about 1%).

4.3 BER Performance of MC-CDMA System

Fig.10 shows the BER performance of MC-CDMA system, where the delay profiles are all the same as those used in the analysis of DS-CDMA system. The frequency domain Rake receiver with no simultaneous other user can achieve the best performance easily, because it can effectively combine the energy of received signal scattered in the frequency domain using a lot of sub-carriers. On the other hand, the performance of orthogonality restoring single-user detection method is poor, although it is insensitive to the number of users. Among three delay profiles, the performance in the 2-path uniform delay profile is slightly better, because there is a less distortion in the frequency domain.

Fig.11 shows the BER performance of the proposed multi-user detection method for the 2-path uniform delay profile. The proposed multi-user detection method is simple and can improve the BER as compared with the single-user detection method. However, the performance gradually degrades as the number of users increases. If more sophisticated (but more complicated) multi-user detection methods such as the Wiener filtering detection[10], the maximum-likelihood detection[7] and the decorrelating interference canceler[11], are employed, the performance can be more improved.

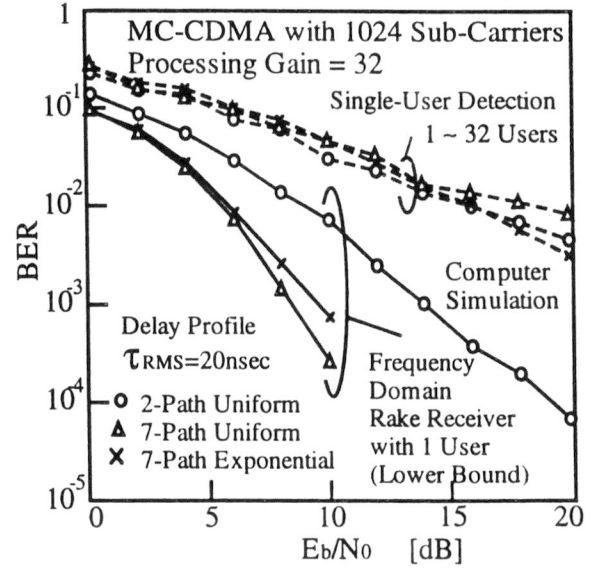


Fig. 10: BER of MC-CDMA System For Single-User Detection and Frequency Domain Rake Methods

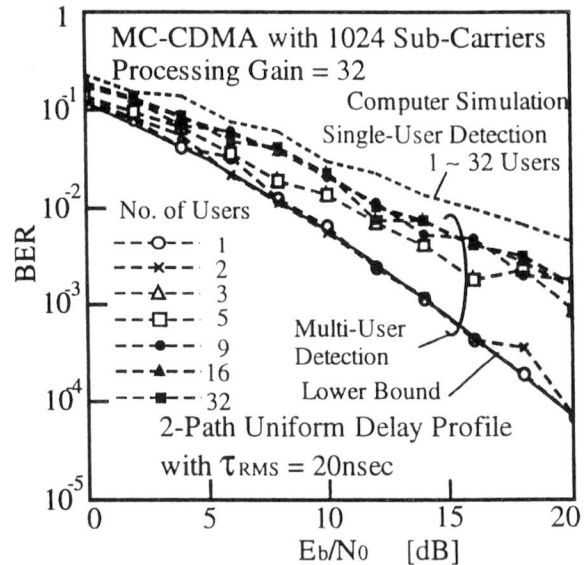


Fig. 11: BER of MC-CDMA System For Multi-User Detection Method (2-Path Uniform Delay Profile)

4.4 BER Comparison of DS-CDMA and MC-CDMA Systems

Fig.12 shows the BER comparison of DS-CDMA and MC-CDMA systems. The best performance of MC-CDMA system agrees well with that of DS-CDMA system. This implies that the frequency domain Rake receiver is equivalent to the time domain Rake receiver for the case of no other user. The next section theoretically proves the equivalence of time domain and frequency domain Rake receivers.

For the performance with 16 users, the MC-CDMA system with the single-user detection method does not work well (but it is insensitive to the number of users). Also, the performance of DS-CDMA system with full-finger Rake receiver is not so good (it becomes worse as the number of users increases).

The performance of DS-CDMA system with non-Rake receiver is much worse than that of MC-CDMA system. Therefore, a Rake receiver could be necessary for the DS-CDMA system.

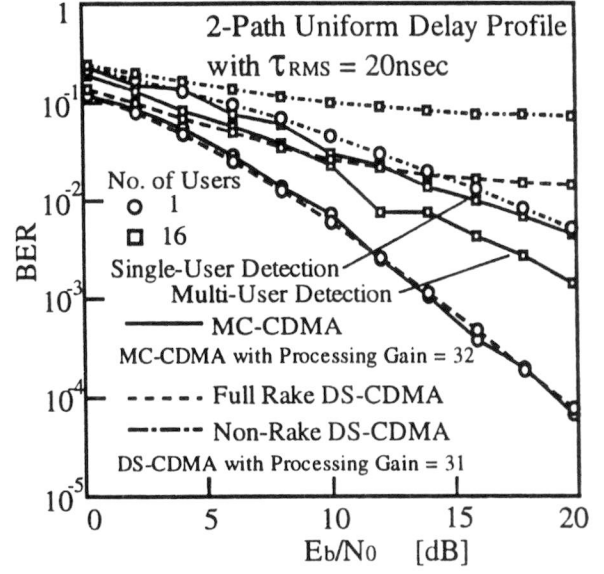


Fig. 12: BER Comparison of DS-CDMA and MC-CDMA Systems (2-Path Uniform Delay Profile)

5 Equivalence of Time Domain DS-CDMA and Frequency Domain MC-CDMA Rake Receivers

As shown in Section 3, the BER of Rake receiver is determined by the eigenvalues of the channel covariance matrix. Therefore, for a multipath delay profile, if the frequency domain covariance matrix has all the same eigenvalues as the time domain covariance matrix, the BER of frequency domain Rake receiver is all the same as that of time domain Rake receiver.

In the FFT, the frequency resolution is determined by the observation period. Therefore, for the multi-carrier modulation with N sub-carriers, N -point DFT is required in the symbol duration T_0 . Assume the following $N \times N$ time domain covariance matrix with the time resolution of T_0/N , for example, for the multipath delay profile shown in Fig.13:

$$\mathbf{M}'_t = \begin{bmatrix} \sigma_1^2 & 0 & \cdots & \cdots & \cdots & 0 \\ 0 & 0 & & & & \vdots \\ \vdots & & \sigma_1^2 & & & \vdots \\ \vdots & & & \sigma_3^2 & & \vdots \\ \vdots & & & & \ddots & 0 \\ 0 & \cdots & \cdots & \cdots & 0 & \ddots \end{bmatrix}, \quad (24)$$

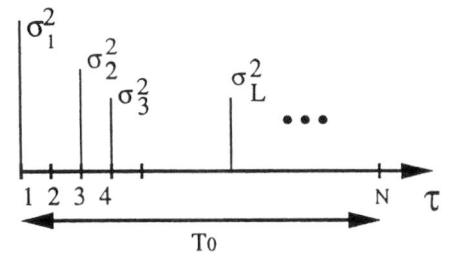


Fig. 13: Multipath Delay Profile

where the non-zero eigenvalues of \mathbf{M}'_t are $\sigma_1^2, \sigma_2^2, \sigma_3^2, \dots, \sigma_L^2$.

Using \mathbf{M}'_t , the frequency domain covariance matrix is written by

$$\mathbf{M}'_f = \mathbf{W}\mathbf{M}'_t\mathbf{W}^*, \quad (25)$$

where \mathbf{W} is the $N \times N$ Discrete Fourier Transform matrix given by

$$\begin{aligned} \mathbf{W} &= \{w^{i,j}\}, \\ w^{i,j} &= e^{j2\pi \frac{ij}{N}}. \end{aligned} \quad (26)$$

We define \mathbf{r}_l as the eigenvector corresponding to the eigenvalue σ_l^2 :

$$\mathbf{M}'_t\mathbf{r}_l = \sigma_l^2\mathbf{r}_l \quad (l = 1, 2, \dots, L). \quad (27)$$

Also, we define \mathbf{z}_l as

$$\mathbf{z}_l = \mathbf{W}\mathbf{r}_l \quad (l = 1, 2, \dots, L). \quad (28)$$

Now, we can theoretically prove that the frequency domain covariance matrix has all the same eigenvalues as the time domain covariance matrix as follows:

$$\begin{aligned} \mathbf{M}'_f\mathbf{z}_l &= \mathbf{W}\mathbf{M}'_t\mathbf{W}^* \cdot \mathbf{W}\mathbf{r}_l \\ &= \mathbf{W}\mathbf{M}'_t\mathbf{r}_l \\ &= \mathbf{W}\sigma_l^2\mathbf{r}_l \\ &= \sigma_l^2\mathbf{W}\mathbf{r}_l \\ &= \sigma_l^2\mathbf{z}_l. \end{aligned} \quad (29)$$

The above equation clearly shows that the eigenvalues of \mathbf{M}'_f are $\sigma_1^2, \sigma_2^2, \sigma_3^2, \dots, \sigma_L^2$.

Also, we can see that *the assumption of independent fading characteristic at each sub-carrier implies a frequency selective fading at each sub-carrier as long as we employ the OFDM signaling*, because it requires N paths uniformly scattered in the symbol duration.

6 Conclusions

This paper has discussed the advantages and disadvantages of DS-CDMA and MC-CDMA systems, and analyzed the BER performance in given frequency selective Rayleigh fading channels.

The MC-CDMA system can accommodate more users than the DS-CDMA system for a given frequency bandwidth, on the other hand, it has to make an extra effort in the FFT window synchronization at the receiver and the linear amplification at the transmitter.

For the DS-CDMA system, the Rake receiver is necessary to improve the BER in frequency selective fading channels. However, from the hardware limitation, it is difficult to use all the received signal energy scattered in the time domain.

The MC-CDMA system can easily combine the signal energy scattered in the frequency domain. However, a multi-user detection method is also necessary.

In the best BER comparison, there is no difference between the DS-CDMA and MC-CDMA systems. If the DS-CDMA system cannot work well for a given channel condition and a given system condition, in other words, a given frequency selectivity and a given processing gain, the MC-CDMA system can be attractive even at the sacrifice of cost for the sub-carrier synchronization, because it can effectively combine the signal energy scattered in the frequency domain for any frequency selectivity and any processing gain using a number of sub-carriers.

Acknowledgement

The authors wish to thank Prof. Y. Bar-Ness of New Jersey Institute of Technology, Dr. J-P. Linnartz of Philips Research and Assist. Prof. M. Okada of Osaka University for their helpful comments and fruitful discussions.

References

- [1] N.Yee, J-P.Linnartz and G.Fettweis : "Multi-Carrier CDMA in Indoor Wireless Radio Networks," Proc. of IEEE PIMRC'93, pp.109-113, Yokohama, Japan, Sept. 1993.
- [2] K.Fazel and L.Papke : "On the Performance of Convolutionally-Coded CDMA/OFDM for Mobile Communication System," Proc. of IEEE PIMRC'93, pp.468-472, Yokohama, Japan, Sept. 1993.
- [3] J.G.Proakis : "Digital Communications," Mc-Graw Hill, 2nd Ed., 1991.
- [4] H.Sari and I.Jeanclaude : "An Analysis of Orthogonal Frequency-Division Multiplexing for Mobile Radio Applications," Proc. of 1994 IEEE VTC'94, pp.1635-1639, Stockholm, Sweden, June 1994.
- [5] P.Monsen : "Digital Transmission Performance on Fading Dispersive Diversity Channels," IEEE Trans. Commun., vol.COM-21, pp.33-39, Jan. 1973.
- [6] M.B.Pursley : "Performance Evaluation for Phase-Coded Spread-Spectrum Multiple-Access Communications-Part I : System Analysis," IEEE Trans. Commun., vol.COM-25, pp.795-799, Aug. 1977.
- [7] K.Fazel : "Performance of CDMA/OFDM for Mobile Communication System," Proc. of IEEE ICUPC'93, pp.975-979, Ottawa, Canada, Oct. 1993.
- [8] N.Yee and J-P.Linnartz : "Controlled Equalization of Multi-Carrier CDMA in an Indoor Rician Fading Channel," Proc. of IEEE VTC'94, pp.1665-1669, Stockholm, Sweden, June 1994.
- [9] S.Hara, M.Mouri, M.Okada and N.Morinaga : "Transmission Performance Analysis of Multi-Carrier Modulation in Frequency Selective Fast Rayleigh Fading Channel," , accepted for publication in Wireless Personal Communications : An International Journal, Special Issue on Multi-Carrier communications, Kluwer Academic Publishers.
- [10] N.Yee and J-P.Linnartz : "Wiener Filtering of Multi-Carrier CDMA in a Rayleigh Fading Channel," Proc. of IEEE PIMRC'94, pp.1344-1347, The Hague, The Netherlands, Sept. 1994.
- [11] Y.Bar-Ness, J-P.Linnartz and X.Lin : "Synchronous Multi-User Multi-Carrier CDMA Communication System with Decorrelating Interference Canceler," Proc. of IEEE PIMRC'94, pp.184-188, The Hague, The Netherlands, Sept. 1994.